

# Tryptophan 2,3-Dioxygenase (TDO) Inhibitors. 3-(2-(Pyridyl)ethenyl)indoles as Potential Anticancer Immunomodulators

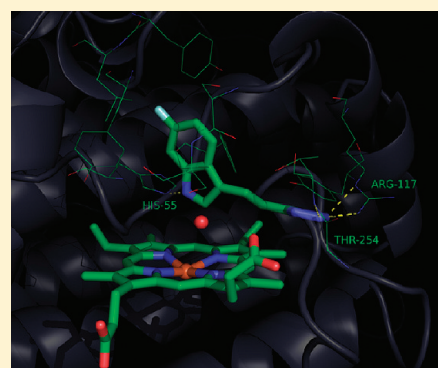
Eduard Dolušić,<sup>†</sup> Pierre Larrieu,<sup>‡</sup> Laurence Moineaux,<sup>†</sup> Vincent Stroobant,<sup>‡</sup> Luc Pilotte,<sup>‡</sup> Didier Colau,<sup>‡</sup> Lionel Pochet,<sup>†</sup> Benoît Van den Eynde,<sup>‡</sup> Bernard Masereel,<sup>†</sup> Johan Wouters,<sup>†</sup> and Raphaël Frédérick<sup>\*,†</sup>

<sup>†</sup>Drug Design and Discovery Center, University of Namur, 61 Rue de Bruxelles, 5000 Namur, Belgium

<sup>‡</sup>Ludwig Institute for Cancer Research, Université Catholique de Louvain, 74 Avenue Hippocrate, 1200 Brussels, Belgium

**S** Supporting Information

**ABSTRACT:** Tryptophan catabolism mediated by indoleamine 2,3-dioxygenase (IDO) is an important mechanism of peripheral immune tolerance contributing to tumoral immune resistance. IDO inhibition is thus an active area of research in drug development. Recently, our group has shown that tryptophan 2,3-dioxygenase (TDO), an unrelated hepatic enzyme also catalyzing the first step of tryptophan degradation, is also expressed in many tumors and that this expression prevents tumor rejection by locally depleting tryptophan. Herein, we report a structure–activity study on a series of 3-(2-(pyridyl)ethenyl)indoles. More than 70 novel derivatives were synthesized, and their TDO inhibitory potency was evaluated. The rationalization of the structure–activity relationships (SARs) revealed essential features to attain high TDO inhibition and notably a dense H-bond network mainly involving His<sub>55</sub> and Thr<sub>254</sub> residues. Our study led to the identification of a very promising compound (**58**) displaying good TDO inhibition ( $K_i = 5.5 \mu\text{M}$ ), high selectivity, and good oral bioavailability. Indeed, **58** was chosen for preclinical evaluation.



## INTRODUCTION

Indoleamine 2,3-dioxygenase (IDO, EC 1.13.11.52) and tryptophan 2,3-dioxygenase (TDO, EC 1.13.11.11) are cytosolic heme dioxygenases that catalyze the oxidative cleavage of the C2–C3 bond of the indolic ring of *L*-tryptophan (*L*-Trp). This reaction is the first and rate-limiting step of the kynurenine pathway of tryptophan catabolism, which eventually leads to the formation of nicotinamide dinucleotide (NAD<sup>+</sup>), a process regarded as the primary biological function of TDO.<sup>1–3</sup> Despite catalyzing the same biochemical reaction and sharing relatively conserved active site regions,<sup>1</sup> the two enzymes share an overall amino acid sequence identity of not more than 10%.<sup>4</sup> TDO was discovered in the 1930s and described as being both eukaryotic and prokaryotic.<sup>5</sup> This enzyme is homotetrameric and almost exclusively found in the liver where it was also first characterized.<sup>6</sup> TDO is highly specific for *L*-Trp and some of its derivatives substituted in the 5- and 6-positions of the indole ring.<sup>7</sup> On the other hand, IDO is monomeric and extrahepatic and shows activity toward a larger collection of substrates, including serotonin, tryptamine, 5-hydroxytryptophan, and melatonin.<sup>2,3</sup> The two enzymes also have different inducers; IDO is inducible by inflammatory stimuli such as interferon- $\gamma$ , while TDO is induced by tryptophan, glucocorticoids, and kynurenine.<sup>2,8</sup>

Since a few years, a growing body of evidence indicated the involvement of IDO in the phenomenon of immune tolerance.

IDO exerts a local immunosuppressive effect on T-lymphocytes partly because of depriving them of *L*-Trp and partly because of the detrimental effect of the *L*-Trp catabolites.<sup>9–13</sup> The observations that many human tumors constitutively express IDO<sup>14</sup> and that an increased level of IDO expression in tumor cells is correlated with poor prognosis for survival in several cancer types<sup>8,15–17</sup> led to the hypothesis that IDO inhibition might enhance the efficacy of cancer treatments.<sup>14,16,18</sup> Indeed, results from *in vitro* and *in vivo* studies have suggested that the efficacy of therapeutic vaccination or chemotherapy may be improved by concomitant administration of an IDO inhibitor.<sup>14,19–21</sup> A number of groups are thus devoting lots of efforts to discover novel inhibitors of this enzyme.<sup>22–26</sup>

Interestingly, our group recently suggested that TDO would also be expressed in many tumor cells including melanoma, colorectal, bladder, hepatic, and breast or lung cancers and demonstrated in a murine model of cancer that this expression of TDO in tumors has an effect similar to the expression of IDO, in that it prevents tumor rejection by locally degrading tryptophan.<sup>27</sup>

Up to now, only a handful of compounds based on the indole or  $\beta$ -carboline scaffolds were reported as possessing TDO inhibitory activity.<sup>28–34</sup> Among these, the fluorindole 680C91<sup>31,33,34</sup>

**Received:** January 25, 2011

**Published:** July 04, 2011

(which is compound **30** in the present work) belonging to the 3-(2-(pyridyl)ethenyl)indole class described by the Wellcome group as combined TDO/5-HT (serotonin) reuptake inhibitors for antidepressant therapy seemed to be the most interesting hit (Figure 1). It is endowed with an excellent *in vitro* inhibitory potency ( $K_i$  of around 30 nM) on liver-extracted TDO, and at 10  $\mu$ M, it is deprived of any activity on 5-HT reuptake, various 5-HT receptors, IDO and monoamine oxidases A and B.<sup>33</sup>

In our work, we aimed to investigate the effect of **30** in a murine cancer model in order to elucidate the exact role of TDO in cancer immune suppression. However, this study failed to afford the expected results presumably because of a low solubility and/or poor bioavailability of **30**. Herein, we present our efforts on the optimization of the TDO inhibitory potency, aqueous solubility, and bioavailability in this series of TDO inhibitors.

To date, only the 3D coordinates of TDO from *Ralstonia metallidurans* (rmTDO)<sup>35</sup> and *Xanthomonas campestris* (xcTDO)<sup>4</sup> were experimentally elucidated. Among these two bacterial strains, xcTDO shares a good sequence identity with the human form (hTDO, 34%),<sup>4</sup> particularly in the active site area, and therefore constitutes an interesting tool to study the binding of inhibitors. The analysis of the interactions stabilizing 6-fluorotryptophan, a substrate analogue cocrystallized in the active site cavity of xcTDO (PDB code 2NW9), reveals essential features stabilizing tryptophan derivatives in the binding cleft (Figure 2a) and notably (i) the stabilization of the indole ring via an H-bond between its NH group and the imidazole moiety of His<sub>55</sub>, (ii) the ionic interaction of the amino group with the heme propionate chain and with the oxygen of a conserved water molecule, and (iii) the interaction of the carboxylate moiety with the guanidinium of Arg<sub>117</sub> and the backbone NH of Thr<sub>254</sub>. Importantly, this structural analysis also suggested an induced-fit behavior of the

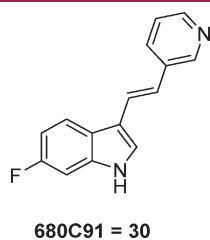
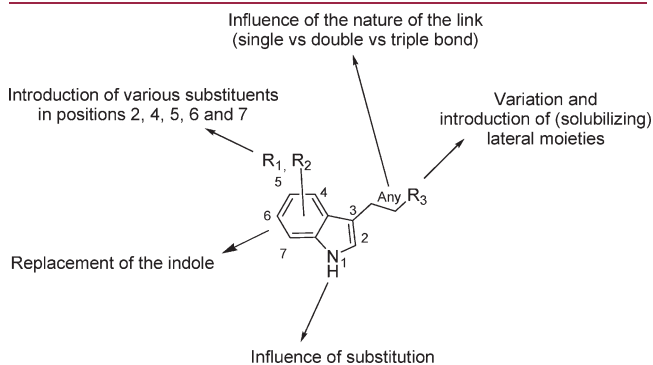


**Figure 1.** Structure of the reported TDO inhibitor 680C91 (**30**).<sup>31,33,34</sup>

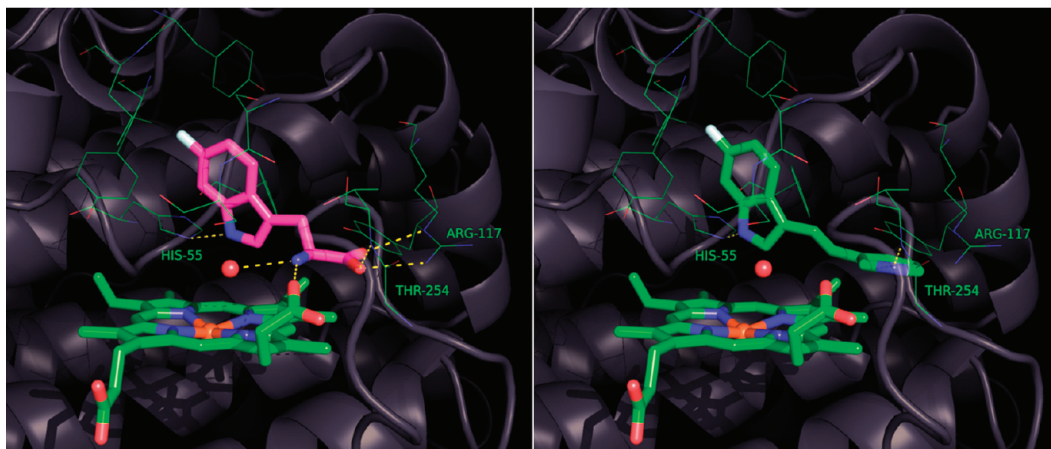
enzyme. Upon recognition of the L-Trp substrate, a complex and extensive network of interactions is established thus stabilizing the active site region. Although this region is exposed to the solvent in the free enzyme, it is completely shielded from the solvent in the substrate–enzyme complex, suggesting that potential ligands would be masked from the solvent upon binding. This has a significant impact in our work, since one of our aims is to improve the aqueous solubility of **30**, and the routine strategy to enhance solubility usually consists of the introduction of a covalently attached solubilizing moiety at positions that are open to solvation. This makes our objective even more challenging, as the attached solubilizing group will be, in our case, buried in the TDO active site upon binding and should therefore be adequately positioned to still allow a proper recognition by TDO.

## RESULTS

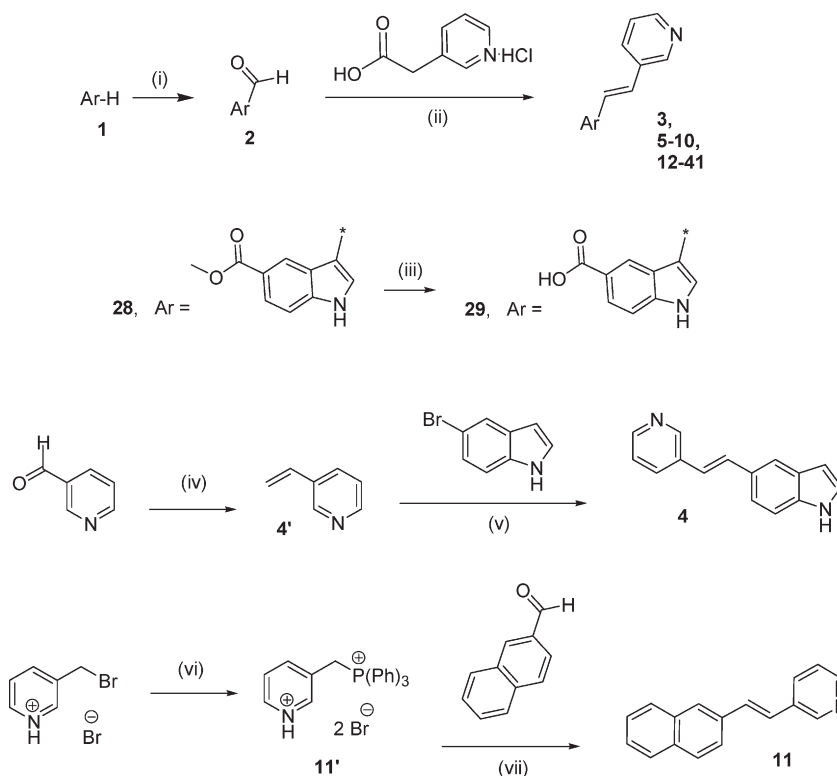
**Rational Design.** An initial docking study of **30** within the xcTDO binding cleft was performed by means of the automated GOLD program<sup>36</sup> and suggested a very similar orientation of the indole moiety compared to the Trp indole, being stabilized through an H-bond with His<sub>55</sub> (Figure 2b). In this orientation, the 3-pyridyl group is projected toward the entrance of the active site and is H-bonded to the Thr<sub>254</sub> NH backbone. On the basis of this modeling study, various modifications of **30** were envisaged, in particular (Figure 3) (i) the replacement of the indole ring, (ii) the introduction of various substituents ( $R_1$ ,  $R_2$ ) in the 1 (NH), 2, 4, 5, 6, and 7 positions around the indole ring, (iii) modification of



**Figure 3.** Envisioned pharmacomodulations around **30**.



**Figure 2.** View of (a, left) 6-fluoro-Trp cocrystallized (PDB code 2NW9) and (b, right) **30** docked inside the TDO binding cleft (pictures made using Pymol).<sup>37</sup>

Scheme 1. Synthetic Scheme for (2-Pyridin-3-yl)vinylarenes<sup>a</sup>

<sup>a</sup> Reagents and conditions: (i)  $\text{POCl}_3/\text{DMF}$ ,  $0^\circ\text{C} \rightarrow$  room temp, 18 h, then 2 M aq NaOH,  $0^\circ\text{C} \rightarrow$  room temp, 2 h; (ii) piperidine,  $\text{Et}_3\text{N}$ , 1,4-dioxane, reflux (18 h to 5 days)<sup>30</sup> or piperidine,  $\text{Et}_3\text{N}$ , MeOH or 1,4-dioxane, microwave (1–12 h), 8–96%; (iii) 2 M aq NaOH, MeOH/THF,  $60^\circ\text{C}$ , 3 h, 65%; (iv)  $\text{TMSCHN}_2$ , *i*-PrOH,  $\text{Ph}_3\text{P}$ , (1,3-dimesityl-2,3-dihydro-1H-imidazol-2-yl)copper(II) chloride,  $60^\circ\text{C}$ , 24 h, 30%; (v)  $\text{Pd}(\text{OAc})_2$ ,  $\text{Ph}_3\text{P}$ , (*i*-Pr)<sub>2</sub>NH, NMP,  $140^\circ\text{C}$ , 18 h, 17%; (vi)  $\text{PPh}_3$ ,  $\text{CH}_3\text{CN}$ , reflux, 7 h, quantitative; (vii) NaH, THF, room temp, 30 min, 69% of a ~1:1 *trans/cis* mixture.

the ethenyl linker, and (iv) modification of the aromatic side chain ( $\text{R}_3$ ). The substituents were chosen with the double objective (i) to derive informative SARs and (ii) to improve the solubility in this series.

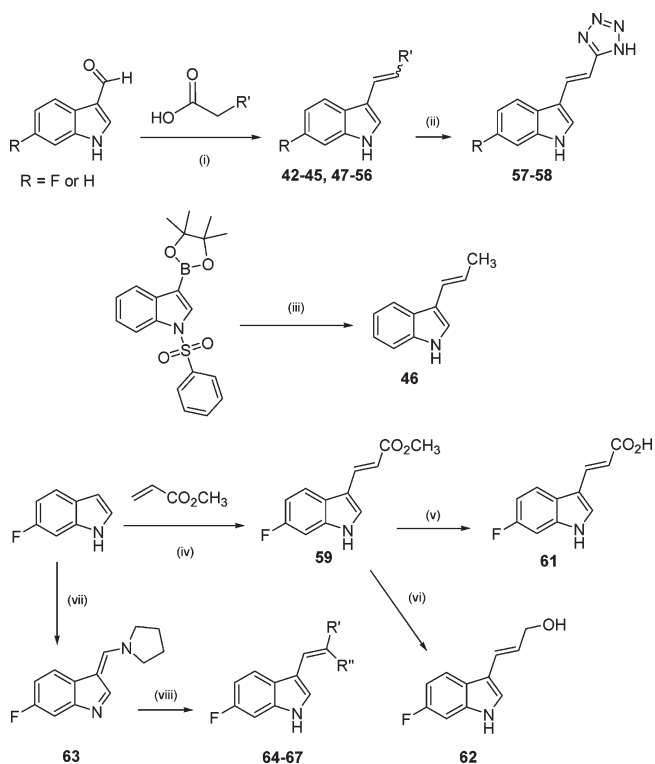
**Chemistry.** Most of the analogues 3–41 of the lead compound (680C91 = 30) were prepared using the same general pathway (Scheme 1).<sup>31</sup> 2-(Pyridin-3-yl)acetic acid hydrochloride was condensed with an appropriate aromatic carbaldehyde under decarboxylative Knoevenagel conditions using either conventional or microwave heating. In all cases, only *trans*-ethene could be isolated as the final product. If the necessary carbaldehyde was not commercially available, it was prepared by a Vilsmeier–Haack formylation of the parent heterocycle. The exception was 5-azaindole carbaldehyde used in the synthesis of compound 6. This reagent was made from commercial 5-azaindole using a sequence described in the literature.<sup>38</sup>

Indole acid 29 was prepared by the saponification of ester 28. Indolic regioisomer 4 was made by a Heck–Mizoroki reaction of 5-bromoindole with 3-vinylpyridine, the latter synthesized from nicotinaldehyde following a literature procedure.<sup>39</sup> Naphthalene analogue 11, along with a roughly equimolar amount of its *cis* isomer, was made according to a Wittig protocol from 3-(bromomethyl)pyridinium bromide<sup>40</sup> and 2-naphthaldehyde.

Compounds 42–45 and 47–56, containing a modified side chain moiety, were synthesized from appropriately substituted indole-3-carbaldehyde following the same strategy as developed for the synthesis of the pyridin-3-yl analogues above using commercial, appropriately substituted acetic acids (Scheme 2). During

the syntheses of acrylonitriles 55 and 56, both the major (55-*trans* and 56-*trans*) and the minor (55-*cis* and 56-*cis*) isomers could be isolated in a molar ratio varying from 2:1 to 3:1. Again, in the other syntheses, only the *trans* isomers were obtained. In the case of phenyl derivative 47, the microwave-promoted reaction had to be performed in dioxane; otherwise, the product was obtained in an inseparable mixture with a significant amount (approximately 1/3 molar) of methyl 3-(6-fluoro-1H-indol-3-yl)-2-phenylacrylate. Tetrazoles 57 and 58 were obtained by [3 + 2] cycloadditions of indole acrylonitriles 55-*trans* and 56-*trans* with aluminum azide preformed in situ as described in the literature.<sup>41,42</sup> Propenylindole 46 was made by a short Suzuki coupling/indole N-deprotection sequence. Indole acrylic ester 59 was obtained by Gaunt's direct regioselective alkenylation<sup>43</sup> of 6-fluoro-1H-indole with methyl acrylate in a very good yield. Saponification of ester 59 gave acid 61, while treating the same starting compound with diisobutyl aluminum hydride gave allylic alcohol 62. Pyrrolidinylmethylene-3H-indole intermediate 63 was prepared from 6-fluoroindole by Vilsmeier–Haack formylation followed by a condensation of the product carbaldehyde with pyrrolidine. This intermediate was converted into several final trisubstituted ethenes (64–67) using chemistry described in the literature.<sup>44</sup>

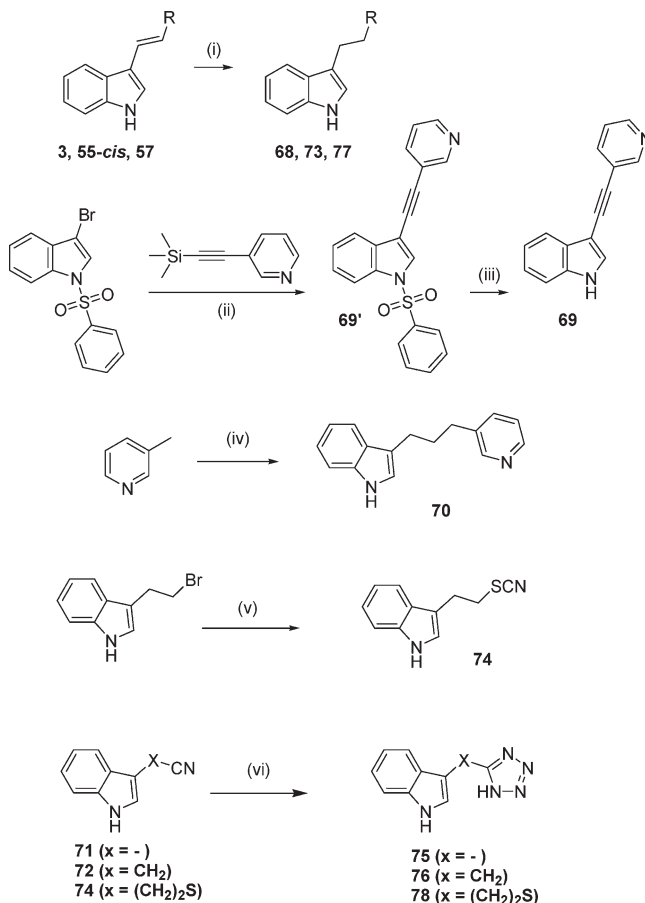
Single-bond tethered compounds 68, 73, and 77 were prepared from appropriate alkenes by catalytic hydrogenation over Pd/C (Scheme 3). Alkyne 69 was made from commercially available N-protected 3-bromoindole which was reacted with 3-((trimethylsilyl)ethynyl)pyridine in a copper-free Sonogashira-type

Scheme 2. Synthetic Scheme for Modifications of the Side Chain<sup>a</sup>

<sup>a</sup> Reagents and conditions: (i) piperidine, Et<sub>3</sub>N, 1,4-dioxane, reflux (24–48 h) or piperidine, Et<sub>3</sub>N, MeOH, microwave, 150 °C (4–12 h), 25–94%; (ii) AlCl<sub>3</sub>/NaN<sub>3</sub>, THF, reflux, 2 h, then compound 55-*trans* or 56-*trans*, reflux, 18 h, 26–64%; (iii) (*E*)-1-bromoprop-1-ene, Pd(PPh<sub>3</sub>)<sub>4</sub>, aq Na<sub>2</sub>CO<sub>3</sub>, toluene, microwave (120 °C), 30 min, then KOH, H<sub>2</sub>O/MeOH, reflux, 18 h, 54%; (iv) Pd(OAc)<sub>2</sub>, Cu(OAc)<sub>2</sub>, DMF/DMSO 9/1, 70 °C, 18 h, 79%; (v) KOH, H<sub>2</sub>O/EtOH, reflux, 1 h, 82%; (vi) DIBAL, toluene, –78 °C, 30 min, 37%; (vii) POCl<sub>3</sub>/DMF, 0 °C → room temp, 18 h, then 2 M aq NaOH, 0 °C → room temp, 2 h, then pyrrolidine, toluene, reflux, 2.5 h, 98%; (viii) RCH<sub>2</sub>R', pyridine, room temp, 1–20 h, 3–96% or RCH<sub>2</sub>R', Et<sub>3</sub>N, EtOH, room temp, 19 h, 81%.

coupling reaction<sup>45</sup> in the presence of tetrahexyl ammonium chloride as the trimethylsilyl group cleaving agent to give N-protected alkyne 69' in a single-pot operation. The N-deprotection of the indole moiety under basic conditions furnished the desired final product in a satisfactory yield. Derivative 70 containing a C3 linker was synthesized by nucleophilic substitution on the corresponding alkyl bromide with carbene prepared in situ from 3-picoline, analogous to literature procedures.<sup>25,26,46</sup> Thiocyanate 74 was obtained by another nucleophilic displacement on the same alkyl bromide and subsequently converted<sup>47</sup> to tetrazole sulfide 78. Two more tetrazoles 75 and 76 with variable linker lengths were made from commercial nitriles 71 and 72 analogous to the compounds 57 and 58.

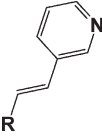
**TDO Inhibition.** The synthesized derivatives were assayed for their ability to inhibit tryptophan degradation and kynurenine production in cells expressing murine TDO (mTDO).<sup>27</sup> Briefly, the assay was performed in 96-well flat bottom plates seeded with  $2 \times 10^5$  cells (P185B-mTDO clone 12) in a final volume of 200  $\mu$ L. The potency of the compounds as TDO inhibitors was first evaluated after overnight incubation of cells at 37 °C in HBSS (Hanks' balanced salt solution) supplemented with 80  $\mu$ M

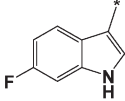
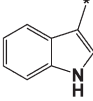
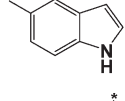
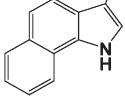
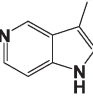
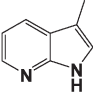
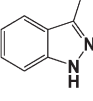
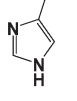
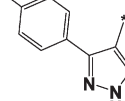
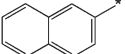
Scheme 3. Synthetic Scheme for Linker Modifications<sup>a</sup>

<sup>a</sup> Reagents and conditions: (i) H<sub>2</sub> (1 atm), 3% Pd/C, EtOH/THF, room temp, 24 h to 3 days, 36–92%; (ii) Pd(OAc)<sub>2</sub>, NaOAc, PPh<sub>3</sub>, (*n*-Hex)<sub>4</sub>NCl, DMF, microwave, 100 °C, 15 min, 62%; (iii) sat. aq NaHCO<sub>3</sub>, MeOH, 60 °C, 72 h, 93%; (iv) LDA, THF/hexanes, –78 to 0 °C, 1 h, then 3-(2-bromoethyl)-1H-indole, THF/hexanes, 0 °C to room temp, 20 h, 75%; (v) KSCN, (*n*-Bu)<sub>4</sub>NBr, THF, reflux, 24 h, quantitative; (vi) AlCl<sub>3</sub>/NaN<sub>3</sub>, THF, reflux, 2 h, then compound 71 or 72, reflux, 21 h, 66–67% or NaN<sub>3</sub>/ZnBr<sub>2</sub>, *i*-PrOH/H<sub>2</sub>O, reflux, 6 h, 70% over two steps.

1-tryptophan and 2, 20, or 200  $\mu$ M of the studied compound. The plates were then centrifuged (10 min, 300g). The supernatant (150  $\mu$ L) was collected and analyzed by HPLC to measure the concentration of residual tryptophan and produced kynurenine. The inhibition of tryptophan degradation and kynurenine production was expressed as a percentage of the values obtained in the absence of inhibitor. A dose–response assay was then performed to determine the IC<sub>50</sub> of the compounds showing at least 30% inhibitory activity at 20  $\mu$ M. To evaluate the TDO/IDO selectivity, the most active compounds were also screened in cells expressing murine IDO. For each compound, the cell viability, expressed as the LD<sub>50</sub>, was evaluated at the end of the incubation period. This global cellular assay is informative for drug development, as it evaluates a combination of the drugs' TDO/IDO inhibitory potency, their cell penetration, their potential cytotoxicity, the inhibition of tryptophan transporters, and the effects of their metabolites. The results are reported in Tables 1–4. As log *D*<sub>7.4</sub> and drug solubility are widely used for drug development, these parameters were

Table 1. TDO Inhibitory Potency of Analogues of 30



Cmpd	R	mTDO IC <sub>50</sub> (μM) <sup>a</sup>	LD <sub>50</sub> (μM) <sup>a</sup>	Calculated <sup>b</sup>	
				LogD <sub>7.4</sub>	Solubility (mg/mL)
680C91 = 30		1	> 80	3.73	0.065
3		1	> 80	3.53	0.21
4		> 200	> 80	3.87	0.15
5		> 200	> 80	4.71	0.0077
6		> 200	> 80	1.42	13.7
7		18	> 80	1.92	1.74
8		> 200	> 80	2.82	0.20
9		> 200	> 80	1.31	6.0
10		> 200	> 80	3.16	0.012
11		> 200	> 80	4.14	0.020

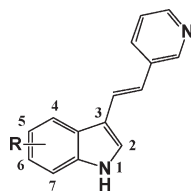
<sup>a</sup> IC<sub>50</sub> and LD<sub>50</sub> values tested in cells transfected with mouse TDO (mTDO). <sup>b</sup> Lipophilicity expressed as log D<sub>7.4</sub> and solubility calculated using software from ACD Labs.<sup>48</sup>

calculated with ACD Labs software to guide the optimization process.

**Replacement of the Indole.** Initially, we investigated the replacement of the indole moiety of the lead **30**, retaining the vinylpyrid-3-yl side chain. In order to preserve the putative

H-bond with His<sub>55</sub> suggested by modeling (see above), hetero-aromatic rings possessing an H-bond donor group, such as 5- or 7-azaindole, indazole, 1*H*-benzo[*g*]indole, imidazole, or phenylpyrazole, were preferentially selected (Table 1). First, removal of the fluorine in the 6-position of the parent **30** (IC<sub>50</sub> = 1 μM)

Table 2. TDO Inhibitory Potency of Indole Derivatives Substituted in the 1, 2, 4, 5, 6, and 7 Positions



compd	R	mTDO IC <sub>50</sub> (μM) <sup>a</sup>	LD <sub>50</sub> (μM) <sup>a</sup>	calculated <sup>b</sup>	
				log D <sub>7,4</sub>	solubility (mg/mL)
3	H	1	>80	3.73	0.21
12	1-N-Me, 6-F	>200	>200	3.45	0.079
13	2-Me	>200	>200	3.57	0.14
14	2-Phenyl	>200	>200	4.27	0.014
15	4-F	10	>80	3.66	0.069
16	4-Cl	>40	40–80	4.2	0.042
17	4-Br	>200	>200	4.29	0.053
18	4-CN	>200	>200	3.41	0.049
19	4-NO <sub>2</sub>	>200	>200	3.27	0.071
20	4-COOMe	>200	>200	3.48	0.13
21	5-F	5	>80	3.58	0.073
22	5-Cl	20	>80	4.03	0.048
23	5-Br	40	20–40	3.73	0.083
24	5-Me	>200	>200	3.95	0.10
25	5-OMe	40	>80	3.03	0.25
26	5-CN	>200	>200	3.41	0.049
27	5-NO <sub>2</sub>	>200	>200	3.46	0.061
28	5-COOMe	>200	>200	3.52	0.13
29	5-COOH	>200	>200	0.13	21.3
30	6-F	1	>80	3.73	0.065
31	6-Cl	20	>40	4.35	0.037
32	6-Br	>200	>200	4.36	0.049
33	6-Me	>200	>200	4.07	0.094
34	6-MeO	>200	>200	3.02	0.25
35	6-OH	>200	>200	2.89	0.54
36	6-COOMe	>200	>200	3.48	0.13
37	7-F	50–100	>400	3.66	0.068
38	7-Cl	>200	>200	3.71	0.064
39	7-Br	>20	20–40	4.29	0.052
40	7-Me	>200	>200	3.53	0.15
41	7-MeO	>200	>200	3.52	0.16

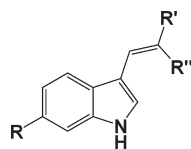
<sup>a</sup> IC<sub>50</sub> and LD<sub>50</sub> values tested in cells transfected with mouse TDO (mTDO). <sup>b</sup> Lipophilicity expressed as log D<sub>7,4</sub> and solubility calculated using software from ACD Labs.<sup>48</sup>

resulted in an equipotent TDO inhibitor (**3**, IC<sub>50</sub> = 1 μM). Regarding the replacement of the indole, apart from compound **7** (IC<sub>50</sub> = 18 μM), bearing a 7-azaindole in place of the indole ring, none of the investigated replacements afforded a compound retaining some TDO inhibitory potency. Surprisingly, even the replacement of the indole with 5-azaindole (**6**) or indazole (**8**) isosteres totally suppressed the activity. These results clearly emphasize the importance of the indole moiety to reach a high TDO inhibitory potency.

**Substitution on the Indole.** Next, we investigated the substitution around the indole ring. As already mentioned, removal of the fluorine in the 6-position of the parent **30** (IC<sub>50</sub> = 1 μM) resulted in an equipotent TDO inhibitor (**3**, IC<sub>50</sub> = 1 μM).

Compared to this unsubstituted compound **3**, the methylation of the indole nitrogen (**12**) completely suppresses the TDO inhibitory potency. This observation supports the putative binding orientation observed by docking (see hereunder), suggesting the stabilization of the indole of **30** via an H-bond with the imidazole of His<sub>55</sub>. In agreement with the modeling study, the introduction of either a methyl (**13**) or a phenyl (**14**) in the 2-position led to inactive compounds. Regarding the substitution of the indole in the 4, 5, 6, or 7 positions, a general trend can be highlighted. Indeed, whatever the position considered, only small and rather lipophilic substituents are tolerated. Generally, the introduction of fluorine in either position led to very potent derivatives (**15**, **21**, **30**, **37**), whereas its replacement by a chlorine

Table 3. TDO Inhibitory Potency of Indole Derivatives with Different Side Chains in the 3-Position



compd	R	R'	R''	mTDO IC <sub>50</sub> (μM) <sup>a</sup>	LD <sub>50</sub> (μM) <sup>a</sup>	calculated <sup>b</sup>	
						log D <sub>7.4</sub>	solubility (mg/mL)
3	H	pyrid-3-yl	H	1	>80	3.53	0.21
30	6-F	pyrid-3-yl	H	1	>80	3.73	0.065
42	H	pyrid-2-yl	H	20	>100	3.39	0.23
43	6-F	pyrid-2-yl	H	3	100–200	3.59	0.072
44	H	pyrid-4-yl	H	20	>100	3.44	0.23
45	6-F	pyrid-4-yl	H	3	200–400	3.65	0.069
46	H	CH <sub>3</sub>	H	>80	>80	3.9	0.25
47	6-F	phenyl	H	40	40–80	4.65	0.0081
48	6-F	naphth-2-yl	H	>200	>200	5.84	0.0031
49	6-F	3-F-phenyl	H	10	40–80	4.73	0.0028
50	6-F	3-Cl-phenyl	H	>200	>200	5.35	0.0016
51	6-F	3-Br-phenyl	H	>200	>200	5.58	0.0018
52	6-F	3-OMe-phenyl	H	10	40–80	4.80	0.0058
53	6-F	3-CN-phenyl	H	1	20–40	4.15	0.0027
54	6-F	3-NO <sub>2</sub> -phenyl	H	3	40–80	4.24	0.0031
55- <i>trans</i>	H	CN	H	13	>80	2.76	0.44
56- <i>trans</i>	6-F	CN	H	3	>80	2.96	0.14
57	H	tetrazole	H	10	>80	−0.035	4.11
58	6-F	tetrazole	H	2	>400	0.15	2.88
59	6-F	COOMe	H	2	40–80	3.42	0.13
60	H	COOH	H	18	>400	−0.59	279.30
61	6-F	COOH	H	3	>400	−0.56	130.6
62	6-F	CH <sub>2</sub> OH	H	80	100	2.34	1.1
64	6-F	phenyl	CN	>80	>80	4.27	0.0066
65	6-F	COOEt	CN	>80	>80	3.66	0.042
66	6-F	COOH	CN	>80	>80	−1.62	745.2
67	6-F	COOH	COOH	>80	>80	−3.37	>1000

<sup>a</sup> IC<sub>50</sub> and LD<sub>50</sub> values tested in cells transfected with mouse TDO (mTDO). <sup>b</sup> Lipophilicity expressed as log D<sub>7.4</sub> and solubility calculated using software from ACD Labs.<sup>48</sup>

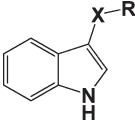
(16, 22, 31, 38) or a bromine (17, 23, 32, 39) resulted in less potent TDO inhibitors. Except for the 5-position, where the introduction of a methoxy seems to be tolerated (25), the substitution by any other groups, including potential solubilizing moieties such as hydroxy (35), nitro (19, 27), methoxy (34, 41), carboxylate (29), and methyl carboxylate esters (20, 28, 36), led to a drastic loss of the TDO inhibitory potency, whatever the position. These observations clearly highlight the highly lipophilic characteristic of the TDO active site in the neighborhood of the heme and its relatively small size. This strongly restrains the number of substituents that can be accommodated. Indeed, regarding this SAR, the most potent derivatives are obtained by substituting the indole in the 5- (21) or 6-position (30) by a fluorine or with the unsubstituted (3) parent compound.

**Pharmacomodulation of the Pyridyl Side Chain.** The replacement of the lateral pyridyl ring was next investigated (Table 3). This pharmacomodulation was driven by two main

objectives: (i) to appraise the importance of the pyrid-3-yl side chain in the stabilization of these derivatives within the TDO binding cleft and (ii) to take advantage of the initial docking of 30 within the TDO binding site to possibly enhance the solubility of these compounds. Indeed, in the putative binding orientation of 30 inside the TDO binding cleft, the 3-pyridyl group is found in the vicinity of the Arg<sub>117</sub> guanidinium so that its replacement with H-bond acceptor groups such as a methyl or an ethyl ester, a nitrile or a methoxy or with a negatively charged group such as a carboxylate or its tetrazolate isostere<sup>49</sup> should provide more soluble compounds that could be further stabilized through ionic interactions in the cleft.

First, the displacement of the nitrogen atom to the 2- (42, 43) or 4-position (44, 45) resulted in a loss of the TDO inhibitory potency in both cases, particularly with the unsubstituted indoles 42 and 44. Moreover, the introduction of a methyl (46), phenyl (47), or a naphth-2-yl (48) instead of the pyrid-3-yl ring strongly decreased the TDO inhibitory potency. These observations

Table 4. TDO Inhibitory Potency of Indole Derivatives with Different Linkers in the 3-Position



Cmpd	X	R	mTDO IC <sub>50</sub> (μM) <sup>a</sup>	LD <sub>50</sub> (μM) <sup>a</sup>	Calculated <sup>b</sup>	
					LogD <sub>7.4</sub>	Solubility (mg/mL)
3			1	> 80	3.73	0.21
68			80	> 80	3.13	0.22
69			6	200-400	3.88	0.0084
70			>200	>200	3.56	0.11
55-trans		CN	13	>80	2.76	0.44
55-cis		CN	> 80	> 80	2.76	0.44
71		CN	>80	>80	2.07	0.55
72		CN	>80	>80	2.63	0.51
73		CN	>80	>80	1.86	0.66
74		CN	44	>80	2.6	0.38
57			10	> 80	-0.035	4.11
75			>80	>80	0.47	3.90
76			>80	>80	-0.37	12.0
77			>80	>80	-0.26	10.0
78			>80	>80	0.2	3.63

<sup>a</sup> IC<sub>50</sub> and LD<sub>50</sub> values tested in cells transfected with mouse TDO (mTDO). <sup>b</sup> Lipophilicity expressed as log D<sub>7.4</sub> and solubility calculated using software from ACD Labs.<sup>48</sup>

clearly support the putative H-bond interaction of the pyrid-3-yl nitrogen atom of **30** with the Thr<sub>254</sub> NH backbone, as suggested by modeling. Interestingly, the introduction of an H-bond acceptor such as a fluorine (**49**), a methoxy (**52**), a nitrile (**53**), a nitro (**54**) in the 3-position of the phenyl group or replacing this group with a methylester (**59**) led systematically to compounds having

a potency similar to that of the parent compound **30**. This reinforces the prerequisite for an H-bond with the Thr<sub>254</sub> NH backbone to properly stabilize the compounds in this series. However, this strategy led to highly lipophilic (3.73 < log D<sub>7.4</sub> < 5.58) and poorly soluble (<0.072 mg · mL<sup>-1</sup>) molecules as deduced from the calculated log D<sub>7.4</sub> and solubility values. Moreover, the



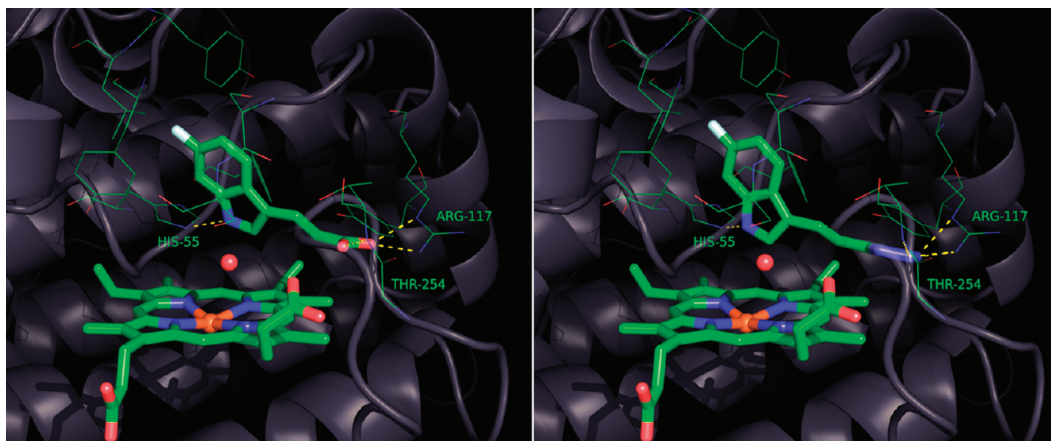


Figure 4. View of (a) **61** and (b) **58** docked inside the TDO binding cleft (pictures made using Pymol).<sup>37</sup>

replacement of the pyrid-3-yl group generated compounds with a significant cellular toxicity ( $LD_{50} \leq 80 \mu M$ ) (Table 3).

The acrylonitriles **55-trans** and **56-trans**, precursors for the synthesis of the tetrazoles **57** and **58**, were revealed to be very potent TDO inhibitors. Their  $IC_{50}$  values are 2.5 and 13.2  $\mu M$ , for the 6-fluoro-substituted **56-trans** and the unsubstituted derivative **55-trans**, respectively. Moreover, these compounds are characterized by a lower lipophilicity ( $\log D_{7.4}$  of 2.76 and 2.96 for **55-trans** and **56-trans**, respectively) and improved solubility (0.44 and 0.14  $mg \cdot mL^{-1}$  for **55-trans** and **56-trans**, respectively) compared to that of their respective parent compounds (for **3** and **30**,  $\log D_{7.4}$  is 3.53 and 3.73 and solubility is 0.21 and 0.065  $mg \cdot mL^{-1}$ , respectively).

The compounds bearing the tetrazolyl (**57**, **58**) and the carboxylic acid (**60**, **61**) moieties on the 3-vinyl linker exhibited a high TDO inhibitory potency, particularly when the indole is substituted in the 6-position by a fluorine (**58**, **61**) ( $IC_{50}$  of 2.0 and 3.2  $\mu M$  for **58** and **61**, respectively). Moreover, compounds **58** and **61** possess improved physicochemical parameters being characterized by a low lipophilicity ( $\log D_{7.4}$  of 0.2 and  $-0.6$ , respectively) and high solubility (2.88 and 130.6  $mg \cdot mL^{-1}$ , respectively). They do not display any cellular toxicity up to 400  $\mu M$  ( $LD_{50} > 400 \mu M$ ). Other strategies that aimed at improving the solubility in this series, such as the replacement of the pyrid-3-yl group with a methyl ester (**59**) or a hydroxymethyl (**62**) or via disubstitution of the vinyl side chain (**64–67**), proved to be unfruitful and generated poorly active or inactive compounds.

Indeed, regarding this pharmacomodulation a general trend is observed. Apart from the pyrid-3-yl analogues **3** and **30**, the introduction of a fluorine atom in the 6-position on the indole moiety leads to a  $\sim 5$ -fold improvement in the TDO inhibitory potency, whatever the nature of the side chain (compare **42** with **43**, **44** with **45**, **55** with **56**, **57** with **58**, and **60** with **61**). This reinforces the importance of the 6-fluoro substituent on the indole in this series to attain a high TDO inhibitory potency.

The analysis of the putative binding orientations of **58** and **61** obtained by modeling confirmed the hypothesis that the introduction of negatively charged groups in the 3-position around the indole ring to interact with the guanidinium side chain of Arg<sub>117</sub> was a viable strategy to enhance solubility without disturbing the stabilization of the compounds in the cleft (Figure 4).

**Modification of the Linker between the Indole and the Pyridine.** Finally, we investigated the influence of the linker between the indole and the lateral chain (Table 4). This analysis

was conducted with unsubstituted indole on one side of the molecule and the most potent side chains on the other side, that is, a pyrid-3-yl, a nitrile, or a tetrazole. As a first observation, whatever the nature of the side chain, the replacement of the *trans*-vinyl linker with an ethyl led in all cases to very poor or inactive derivatives (compare **3**, **55-trans**, and **57** with **68**, **73**, and **77**, respectively). Introducing an acetylene linker afforded compound **69** that is less potent but still relatively active ( $IC_{50} = 6 \mu M$ ). This compound is, however, characterized by a relatively high lipophilicity ( $\log D_{7.4} = 3.88$ ) and a poor predicted solubility (0.0084  $mg/mL$ ). Interestingly, the geometry of the double bond also seems to be crucial for the activity, as the *cis*-nitrile isomer (**55-cis**) is completely inactive compared to its *trans* derivative (**55-trans**).

Regarding the length of the linker, its elongation to a propyl (**70**) or an ethylsulfanyl (**74**, **78**) led to poorly active or inactive compounds, whereas its removal (**71**, **75**) or replacement with a shorter methylene linker (**72**, **76**) also led to inactive derivatives. This study thus demonstrates the rather limited number of possibilities regarding the nature of the linker between the indole and the lateral group. This linker should preferentially be a *trans* double bond or possibly an acetylene to properly orient the side chain in the TDO binding cleft.

**Detailed Physicochemical and Kinetic Analyses on 58 and 61.** On the basis of their good TDO inhibitory potency and their promising theoretical physicochemical parameters ( $\log D_{7.4}$  and solubility), two compounds, tetrazole **58** and carboxylic acid **61**, were selected for further analyses. First, their solubility was experimentally confirmed in phosphate buffer at pH 7.4. Both compounds showed a higher solubility ( $>300 \mu M$ ) than **30** (92  $\mu M$ ) (Table 5). Their stability was also evaluated in the same conditions (PBS, pH 7.4). After 1.5 h of incubation, the recovery of both **58** and **61** was  $\sim 93\%$ , whereas it was only  $\sim 68\%$  for **30**.

Detailed kinetic experiments were then conducted with **30**, **58**, and **61** in order to elucidate their mechanism of TDO inhibition. To this end, a colorimetric test adapted from the protocol previously reported for IDO assays was utilized.<sup>14</sup> In these experiments, extracts of *E. coli* overexpressing recombinant human TDO (hTDO) were used. Briefly, the reaction was initiated by addition of the extract (10  $\mu L$ ,  $\sim 3 \mu g$  of total proteins) to 190  $\mu L$  of prewarmed reaction mixture containing phosphate buffer (50 mM, pH 7.5), ascorbic acid (20 mM), methylene blue (10  $\mu M$ ), bovine catalase (500 IU  $\cdot mL^{-1}$ ), L-Trp at various concentrations with (or without) an inhibitor. The reaction was conducted at 37 °C for 2 and

4 min, stopped by addition of trichloroacetic acid (30% w/v, 40  $\mu\text{L}$ ), and the mixture was incubated at 65  $^{\circ}\text{C}$  for 30 min to allow the conversion of *N*-formylkynurenine into kynurenine. The kynurenine production was quantified by UV absorption at 480 nm following the addition of Ehrlich's reagent. A standard curve was made with pure kynurenine. The rate of catalysis was calculated from the increase of kynurenine concentration between 2 and 4 min.

The Michaelis–Menten constant ( $K_M$ ) of the recombinant hTDO was evaluated at 167  $\mu\text{M}$ . Interestingly, this study suggested a substrate inhibition of TDO at high Trp concentration ( $K_i = 11.5 \text{ mM}$ ). Therefore, the inhibition kinetics were performed at *L*-Trp concentrations not exceeding 800  $\mu\text{M}$ . At these concentrations, *L*-Trp induced TDO inhibition is not significant.

A competitive inhibition profile of hTDO was observed for the three molecules (Table 5, Figure 5). In this assay, compounds **58** ( $K_i = 5.6 \mu\text{M}$ ) and **61** ( $K_i = 32.4 \mu\text{M}$ ) are respectively about 7-fold and 40-fold less potent than parent compound **30** ( $K_i = 0.88 \mu\text{M}$ ).

**Bioavailability.** Following these promising results, we assessed the oral bioavailabilities of **58** and **61** in mice and compared them with that of **30**. Briefly, **30**, **58**, and **61** were

**Table 5.** TDO Inhibition Kinetics, Experimental Solubility, and Stability for Compounds **30**, **58**, and **61**

compd	$K_i(\text{hTDO})^a$ ( $\mu\text{M}$ )	solubility in		stability	
		PBS, pH 7.4, at room temp( $\mu\text{M}$ )	after 1.5 h in PBS, pH 7.4)	(% remaining compd	after 1.5 h in PBS, pH 7.4)
<b>30</b>	0.88 [0.76–0.99]	92	67.6 $\pm$ 1.4		
<b>58</b>	5.6 [4.79–6.48]	>300	93.3 $\pm$ 1.9		
<b>61</b>	32.4 [31.30–41.58]	>300	92.9 $\pm$ 0.64		

<sup>a</sup>On crude hTDO extract. 95% confidence intervals in brackets.

dissolved in water and given ad libitum to DBA/2 mice in the drinking water (1  $\text{mg}\cdot\text{mL}^{-1}$ ). The average daily water uptake was 4.0 mL/mouse. This corresponds to a daily dose of 160  $\text{mg}\cdot\text{kg}^{-1}$ . The plasma concentration of each inhibitor, *L*-Trp, and kynurenine was then measured at days 0, 1, 2, and 7.

Following administration of **30** (160  $\text{mg}\cdot\text{kg}^{-1}\cdot\text{day}^{-1}$ ), only a very low plasma concentration (0.1  $\mu\text{M}$ ) is detected at day 7. Regarding **61**, the plasma concentrations ranged between 1.4 and 18  $\mu\text{M}$ . This suggests that both **30** and **61** undergo rapid elimination and/or metabolism. In contrast, higher plasma concentrations of **58** were detected (60–136  $\mu\text{M}$ ), suggesting a high oral bioavailability in mouse.

**Selectivity Profile of 58.** The promising TDO inhibitory potency, physicochemical parameters, and bioavailability profile of **58** prompted us to further explore this compound, notably regarding its selectivity. In Table 6 are summarized the results regarding the inhibitory potency of **58** on IDO and types A and B monoamine oxidase (MAO), its ability to bind various receptors such as the adrenergic ( $\alpha_1$ – $\alpha_2$  and  $\beta_1$ – $\beta_2$ ), dopamine ( $D_1$ – $D_{2s}$ ), melatonin ( $h\text{MT}_1$ ), and serotonin ( $h5\text{-HT}_{1A}$ ,  $h5\text{-HT}_{1B}$ ,  $h5\text{-HT}_{2A}$ ,  $h5\text{-HT}_{2B}$ ,  $h5\text{-HT}_{3}$ ,  $h5\text{-HT}_{5A}$ ,  $h5\text{-HT}_{6}$ ,  $h5\text{-HT}_7$ ) receptors as well as various transporters (norepinephrine (NE), dopamine (DA) and serotonin (5-HT)). As a result, **58** proved to be highly selective for TDO as, at 10  $\mu\text{M}$ , none of the investigated systems are significantly inhibited. Interestingly, **58** does not display any inhibitory potency on IDO, although both IDO and TDO catalyze the same reaction on tryptophan. The 5-HT transporter is the only target that is weakly inhibited at this concentration (26% inhibition at 10  $\mu\text{M}$ ). Tetrazole **58** thus displays an excellent selectivity profile.

Following these encouraging results, an *in vivo* efficacy study of **58** in mice was considered to decipher the exact role of TDO in cancer immunosuppression. In this work, mice are immunized and challenged and **58** is administered in the drinking water. We observed that systemic treatment of immunized mice with **58** at

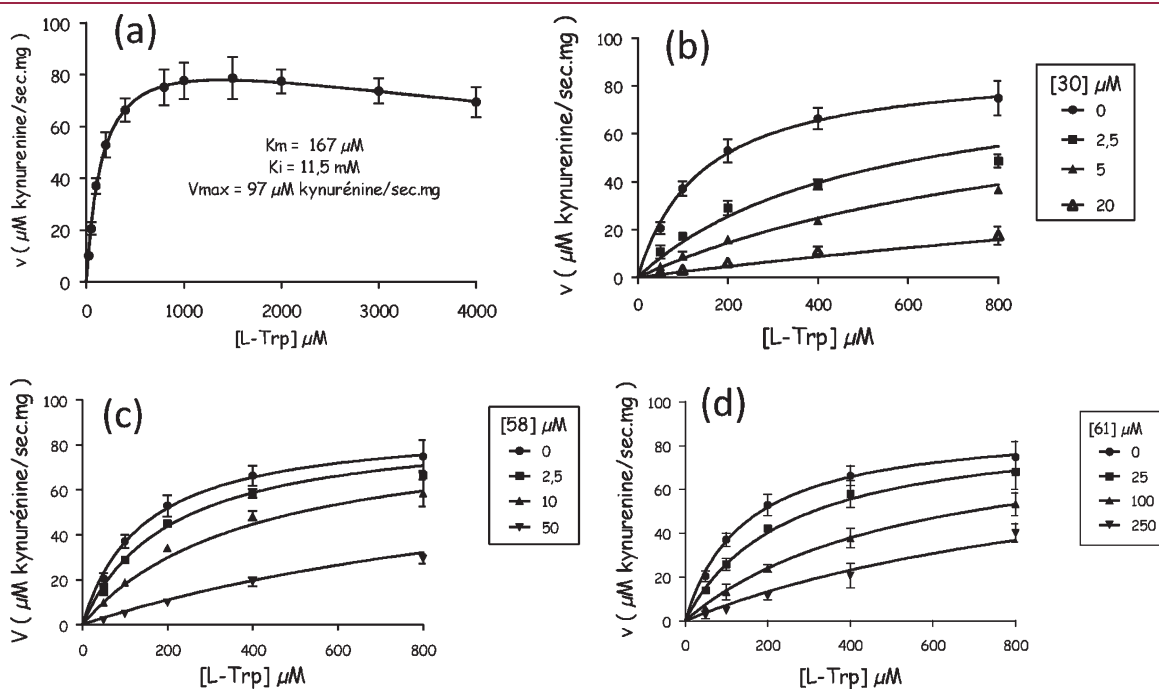


**Figure 5.** Initial velocity vs *L*-Trp concentration plot for the reaction catalyzed by TDO without (a) and with different concentrations of **30** (b), **58** (c), and **61** (d).

Table 6. Selectivity Data for 58

enzyme or receptor	radioligand	ref compd ( $K_i$ , nM)	% inhibition <sup>a</sup> at 10 $\mu$ M
IDO		1-MT (40,000)	<10
MAO-A		harmine (17)	<10
MAO-B		isatine (33)	<10
$\alpha_1$ (nonselective)	[ <sup>3</sup> H]prazosin	prazosin (0.071)	<10
$\alpha_2$ (nonselective)	[ <sup>3</sup> H]RX821002	yohimbine (33)	<10
$\beta_1$	[ <sup>3</sup> H](–)-CGP12177	atenolol (170)	14
$\beta_2$	[ <sup>3</sup> H](–)-CGP12177	ICI 118551 (0.13)	<10
$D_1$	[ <sup>3</sup> H]SCH23390	SCH23390 (0.11)	<10
$D_{2s}$	[ <sup>3</sup> H]methyl-spiperone	(+)-butaclamol (0.50)	<10
$MT_1$	[ <sup>125</sup> I]2-iodomelatonin	melatonin (0.37)	<10
$5-HT_{1A}$	[ <sup>3</sup> H]8-OH-DPAT	8-OH-DPAT (0.17)	<10
$5-HT_{1B}$	[ <sup>125</sup> I]CYP	serotonin (14)	<10
$5-HT_{2A}$	[ <sup>3</sup> H]ketanserin	ketanserin (0.28)	<10
$5-HT_{2B}$	[ <sup>125</sup> I]( $\pm$ )-DOI	( $\pm$ )-DOI (2.0)	<10
$5-HT_3$	[ <sup>3</sup> H]BRL43694	MDL72222 (3.9)	<10
$5-HT_{5A}$	[ <sup>3</sup> H]LSD	serotonin (170)	<10
$5-HT_6$	[ <sup>3</sup> H]LSD	serotonin (84)	<10
$5-HT_7$	[ <sup>3</sup> H]LSD	serotonin (0.13)	<10
(h) NE transporter	[ <sup>3</sup> H]nisoxetine	protriptyline (2.3)	<10
(h) DA transporter	[ <sup>3</sup> H]BTCP	BTCP (2.2)	<10
(h) 5-HT transporter	[ <sup>3</sup> H]imipramine	imipramine (0.77)	26

<sup>a</sup> % inhibition relates to % enzyme inhibition for IDO and MAO and % inhibition of control specific binding for the investigated receptors.

160 (mg/kg)/day prevented the growth of TDO-expressing P815 tumor cells. Moreover, mice treated with 58 did not show obvious signs of toxicity. This work is still under progress and will be detailed in a forthcoming publication.

## DISCUSSION AND CONCLUSIONS

Cancer immunotherapy constitutes a promising approach for cancer treatment. However, it is also becoming clear that an important limitation of this strategy results from the ability of some solid tumors to resist immune rejection. A variety of mechanisms can account for such resistance. One of these mechanisms is based on tryptophan catabolism by IDO, which is frequently expressed in tumors. Lately, we demonstrated in a preclinical model that rejection of IDO-expressing tumors was promoted by systemic treatment with an IDO inhibitor.<sup>14</sup> The search for IDO inhibitors that can be used clinically is the focus of intense efforts.<sup>23–26,50,51</sup> Recently, we have also shown<sup>27</sup> that tumors may also use another pathway to catabolize tryptophan and to resist immune rejection, notably the expression of tryptophan 2,3-dioxygenase (TDO), an unrelated enzyme catalyzing the same reaction and exclusively found in the liver.

In this work we aimed to improve a series of compounds initially reported as TDO inhibitors and characterized by a limited efficacy and oral bioavailability that prevent their use in vivo, with a view to decipher the exact role of TDO in tumoral immunosuppression. A complete SAR study was thus undertaken with the objectives to enhance the activity, the solubility, and the bioavailability in this series. Although the reported SARs undoubtedly shed light on the prerequisites for TDO inhibition, notably a dense H-bond network mainly involving His<sub>55</sub> and Thr<sub>254</sub> residues, the study also suggests that TDO is not necessarily easily druggable and that the design of TDO inhibitors is thus certainly not straightforward, as the enzyme seems to be very

susceptible to small modifications of the inhibitor. In fact, despite relatively complete SARs that were drawn, it has not been possible to strongly improve TDO inhibitory potency in the series. Yet our testing involves a cell-based assay where membrane permeation could be an uncrossing hurdle for some molecules. At least, kinetic experiments, performed on crude TDO extracts, allow good comparison of the two most promising derivatives in this work, 58 and 61, with the parent compound 30. These experiments revealed a common competitive inhibition profile with a slightly weaker TDO inhibitory potency for 58 and 61. But interestingly, both compounds show excellent solubility and stability parameters, particularly 58. Indeed, the oral bioavailability of 58 and 61 was assessed and allowed identifying 58 as the most promising candidate. This compound moreover proved to be highly selective for TDO. It has no significant inhibition of any enzymes or receptors investigated. Altogether, this study led to the identification of the first potent, selective, and bioavailable TDO inhibitor (58). This compound was chosen for further in vivo preclinical trials in mice to decipher the exact role of TDO in cancer immunosuppression.

## EXPERIMENTAL PART

**Chemistry.** All chemical reagents and solvents were used as obtained from commercial sources (Sigma Aldrich, Acros, Maybridge, Apollo, Fisher Scientific, Biosolve). (*E*)-3-(1*H*-Indol-3-yl)acrylic acid (60), 1*H*-indole-3-carbonitrile (71), and 2-(1*H*-indol-3-yl)acetonitrile (72) were purchased from Sigma Aldrich. All reactions were performed under an inert argon (Alphagaz 2) atmosphere, unless stated otherwise. Melting points were determined with a Büchi B-540 capillary melting point apparatus in open capillaries and are uncorrected. Thin layer chromatography (TLC) was performed on silica gel plates (60F<sub>254</sub>, 0.2 mm thick, Merck) with visualization under ultraviolet light (254 and 365 nm). <sup>1</sup>H NMR spectra were recorded in DMSO-*d*<sub>6</sub> solution on a

Jeol JNM EX 400 spectrometer at 400 MHz with tetramethylsilane (TMS) as internal standard.  $^{13}\text{C}$  spectra were recorded on the same spectrometer in DMSO- $d_6$  solution at 100 MHz. Chemical shifts ( $\delta$ ) are expressed in ppm downfield from tetramethylsilane. The microwave-assisted syntheses were carried out in an Initiator 16 single-mode microwave instrument producing controlled irradiation at 2.450 GHz (BiotageAB, Uppsala, Sweden). Reaction times refer to hold times at the temperatures indicated, not to total irradiation times. The temperature was measured with an IR sensor on the outside of the reaction vessel. Elemental analyses (C, H, N) were performed on a Thermo Finnigan-FlashEA 1112 apparatus. Analytical LC/MS analyses were performed on an Agilent 1100 series HPLC coupled with an MSD Trap SL system using UV detection at 254 and 361 nm. Mass spectra were recorded using electron spray ionization (ESI) operating in positive mode, unless stated otherwise. The following method was applied: injection of 10  $\mu\text{L}$  of a 20  $\mu\text{g}\cdot\text{mL}^{-1}$  acetonitrile solution onto a  $\text{C}_{18}$  3.5  $\mu\text{m}$  Zorbax SB column (100 mm  $\times$  3 mm); separation using a gradient (flow rate of 0.5  $\text{mL}\cdot\text{min}^{-1}$ ) of acetonitrile in acetic acid (0.1% v/v in water) from 5% to 95% acetonitrile over 5 min, holding for 3 min, then reversing to 5% acetonitrile within 0.1 min and holding for an additional 5.4 min. Automated flash chromatography was performed on a Biotage AB SP1 system equipped with prepacked flash KP-Sil silica cartridges. The following gradient of ethyl acetate in cyclohexane (unless stated otherwise) was used for elution: the elution started with an ethyl acetate/cyclohexane ratio of 12/88 for one column volume (CV); the ratio increased to 62/38 over 5 CV, kept for 1 CV, then increased to 100/0 over 7 CV, and finally kept at this value over 5 CV. The product detection was by UV absorption at 254 and 320 nm. The products were precipitated by concentration of the pooled column fractions combined with the addition of cyclohexane. The precipitate formed was filtered off, washed twice with cyclohexane, and dried at 40  $^{\circ}\text{C}$  in vacuo to yield an analytically pure sample. All new compounds were determined to be >95% pure by LC/MS. The yields reported refer to combined yields of chromatographically and spectroscopically pure product fractions, and crops were recovered from mother liquors.

**General Synthetic Procedures.** *Method A (Knoevenagel Condensation by Conventional Heating).* A round-bottom flask was charged with dioxane (3 mL), pyrid-3-ylacetic acid hydrochloride or another active methylene compound as indicated (1.5 mmol), and triethylamine (535  $\mu\text{L}$ , 3.8 mol, unless stated otherwise), and the resulting mixture was stirred for approximately 10 min at room temperature. Suitably substituted 1H-indole-3-carbaldehyde (1.0 mmol, either from a commercial source or prepared by Vilsmeier–Haack formylation of the commercial 3-nonsubstituted indole according to the literature procedure,<sup>52</sup> where this product was used crude in the next step) and piperidine (220  $\mu\text{L}$ , 2.2 mmol) were added, and the mixture (typically a yellow suspension that darkens to orange as the reaction progresses) was stirred at reflux temperature for the reaction time indicated. In some cases where the reaction progress was slow (as monitored by TLC in ethyl acetate/cyclohexane 2:1), a piperidine aliquot was added, typically at a reaction time of approximately 24 h. Upon completion of the reaction, the mixture was diluted with ethyl acetate and evaporated on silica. This sample was loaded onto a silica column, and the title product was purified by flash chromatography and crystallized from the pooled column fractions as described above.

*Method B (Knoevenagel Condensation by Microwave Heating).* Method B is analogous to method A except that methanol (3 mL) was used as the solvent instead of dioxane (in this case the reaction mixture was typically a clear solution from the beginning) and microwave heating at 150  $^{\circ}\text{C}$  in a sealed tube was applied for the reaction time indicated. 6-Fluoro-1H-indole-3-carbaldehyde (163 mg, 1 mmol) was used as the starting material in all cases.

*Method C (Tetrazole Synthesis).* A literature procedure<sup>41,42</sup> was followed: anhydrous aluminum chloride (1.05 mol equiv) was suspended

in dry tetrahydrofuran (THF, 1 mL/mmol of starting nitrile) at 0  $^{\circ}\text{C}$ . Sodium azide (2.80 mol equiv) was added, the ice/water bath was removed, and the off-white suspension was stirred at the reflux temperature for 2 h. Upon brief cooling of the mixture, a nitrile (1 mol equiv) was added. The reaction mixture was stirred at reflux temperature for the reaction time indicated. The resulting suspension was cooled, poured into 1 M aqueous citric acid, and extracted several times with ethyl acetate. The combined organic layers were washed with brine and dried over  $\text{MgSO}_4$ . Purification by flash chromatography followed by crystallization as described above furnished the title product.

**(E)-3-(2-Pyridin-3-ylvinyl)-1H-indole (3).**<sup>31</sup> **3** was prepared with general synthetic method A, with reaction time of 18 h. Yellow ochre powder, 190 mg (86%). Mp 191–192  $^{\circ}\text{C}$ . LC/MS  $t_{\text{R}} = 5.2$  min,  $m/z$  [ $\text{MH}^+$ ] 221.  $^1\text{H}$  NMR  $\delta$  11.38 (1H, bs, indole-H1), 8.72 (1H, d,  $J = 1.8$  Hz, ArH), 8.34 (1H, dd,  $J = 4.6, 1.4$  Hz, ArH), 8.01 (1H, d,  $J = 7.6$  Hz, ArH), 7.98 (1H, d,  $J = 8.0$  Hz, ArH), 7.65 (1H, bs, ArH), 7.53 (1H, d,  $J = 16.7$  Hz, HC=CH), 7.40 (1H, d,  $J = 8.0$  Hz, ArH), 7.32 (1H, dd,  $J = 7.9, 4.7$  Hz, ArH), 7.05–7.15 (3H, m, 2 ArH, HC=CH).  $^{13}\text{C}$  NMR  $\delta$  148.0, 147.5, 137.6, 134.8, 132.0, 127.3, 125.6, 125.2, 124.2, 122.4, 120.5, 120.4, 120.0, 114.1, 112.5.

**(E)-6-Fluoro-3-(2-pyridin-3-ylvinyl)-1H-indole (30)**<sup>31,33,34</sup>. **30** was prepared with general synthetic method A, with reaction time of 18 h. Yellow powder, 229 mg (96%). Mp 180–181  $^{\circ}\text{C}$ . LC/MS  $t_{\text{R}} = 5.5$  min,  $m/z$  [ $\text{MH}^+$ ] 239.  $^1\text{H}$  NMR  $\delta$  11.43 (1H, bs, indole-H1), 8.72 (1H, d,  $J = 1.4$  Hz, ArH), 8.34 (1H, d,  $J = 4.8$  Hz, ArH) 8.00 (2H, m, 2 ArH), 7.65 (1H, s, ArH), 7.50 (1H, d,  $J = 16.7$  Hz, HC=CH), 7.33 (1H, dd,  $J = 7.9, 4.7$  Hz, ArH), 7.18 (1H, dd,  $J = 9.8, 2.3$  Hz, ArH), 7.07 (1H, d,  $J = 16.7$  Hz, HC=CH), 6.96 (1H, dt,  $^3J = 9.2$  Hz,  $^4J = 2.4$  Hz, ArH).  $^{13}\text{C}$  NMR  $\delta$  159.6 (d,  $J_{\text{CF}} = 234.6$  Hz), 148.1, 147.7, 137.6 (d,  $J_{\text{CF}} = 12.4$  Hz), 134.7, 132.1, 127.7 (d,  $J_{\text{CF}} = 2.9$  Hz), 124.7, 124.2, 122.5, 121.5 (d,  $J_{\text{CF}} = 10.5$  Hz), 120.4, 114.2, 108.7 (d,  $J_{\text{CF}} = 23.8$  Hz), 98.5 (d,  $J_{\text{CF}} = 24.8$  Hz).

**(E)-3-[2-(3-Chlorophenyl)vinyl]-6-fluoro-1H-indole (50).** **50** was synthesized from 3-chlorophenylacetic acid and without triethylamine using the general synthetic method B, with reaction time of 6 h. Yellowish solid, 223 mg (82%). Mp 153–155  $^{\circ}\text{C}$ . LC/MS  $t_{\text{R}} = 7.6$  min,  $m/z$  [ $\text{MH}^+$ ] 272, 274.  $^1\text{H}$  NMR  $\delta$  11.41 (1H, bs, indole-H1), 8.01 (1H, dd,  $J = 8.7, 5.5$  Hz, ArH), 7.64 (1H, d, overlapped, ArH), 7.63 (1H, d, overlapped, ArH), 7.50 (1H, d, overlapped, ArH), 7.47 (1H, d, overlapped, HC=CH), 7.32 (1H, t,  $J = 7.9$  Hz, ArH), 7.16–7.20 (2H, overlapped, 2 ArH), 7.05 (1H, d,  $J = 16.7$  Hz, HC=CH), 6.95 (1H, dt,  $^3J = 9.2$  Hz,  $^4J = 2.3$  Hz, ArH).  $^{13}\text{C}$  NMR  $\delta$  159.5 (d,  $J_{\text{CF}} = 234.6$  Hz), 141.4, 137.5 (d,  $J_{\text{CF}} = 12.4$  Hz), 134.0, 130.9, 127.8, 126.4, 125.5, 124.6, 124.4, 122.5 (2C), 121.6 (d,  $J_{\text{CF}} = 10.5$  Hz), 114.1, 108.6 (d,  $J_{\text{CF}} = 23.8$  Hz), 98.5 (d,  $J_{\text{CF}} = 25.8$  Hz).

**(Z)-3-(6-Fluoro-1H-indol-3-yl)acrylonitrile (56-cis) and (E)-3-(6-fluoro-1H-indol-3-yl)acrylonitrile (56-trans).** **56-trans** was synthesized from cyanoacetic acid using 2.5 mmol of triethylamine. General synthetic method B was used, with reaction time of 10 h. **56-cis**: white powder, 26 mg (14%). Mp 144–145  $^{\circ}\text{C}$ . LC/MS  $t_{\text{R}} = 5.9$  min,  $m/z$  [ $\text{MH}^+$ ] 187.  $^1\text{H}$  NMR  $\delta$  11.90 (1H, bs, indole-H1), 8.17 (1H, s, indole-H2), 7.82 (1H, dd,  $J = 8.7, 5.3$  Hz, ArH), 7.64 (1H, d,  $J = 11.8$  Hz, HC=CH), 7.26 (1H, dd,  $J = 9.8, 2.3$  Hz, ArH), 6.99 (1H, dt,  $^3J = 9.2$  Hz,  $^4J = 2.3$  Hz, ArH), 5.45 (1H, d,  $J = 11.8$  Hz, HC=CH).  $^{13}\text{C}$  NMR  $\delta$  159.9 (d,  $J_{\text{CF}} = 235.5$  Hz), 141.4, 136.1 (d,  $J_{\text{CF}} = 12.4$  Hz), 128.1, 123.8, 120.3, 120.2 (d,  $J_{\text{CF}} = 10.5$  Hz), 111.7, 109.6 (d,  $J_{\text{CF}} = 24.8$  Hz), 98.9 (d,  $J_{\text{CF}} = 24.8$  Hz), 88.5. **56-trans**: yellow powder, 69 mg (37%). Mp 170–172  $^{\circ}\text{C}$ . LC/MS  $t_{\text{R}} = 5.8$  min,  $m/z$  [ $\text{MH}^+$ ] 187.  $^1\text{H}$  NMR  $\delta$  11.85 (1H, bs, indole-H1), 7.90 (1H, dd,  $J = 8.8, 5.4$  Hz, ArH), 7.85 (1H, s, indole-H2), 7.68 (1H, d,  $J = 16.7$  Hz, HC=CH), 7.23 (1H, dd,  $J = 9.9, 2.5$  Hz, ArH), 6.98 (1H, dt,  $^3J = 9.3$  Hz,  $^4J = 2.3$  Hz, ArH), 6.05 (1H, d,  $J = 16.7$  Hz, HC=CH).  $^{13}\text{C}$  NMR  $\delta$  159.8 (d,  $J_{\text{CF}} = 235.5$  Hz), 144.5, 137.9 (d,  $J_{\text{CF}} = 12.4$  Hz), 132.5, 121.8, 121.6 (d,  $J_{\text{CF}} = 10.5$  Hz), 121.0, 112.6, 109.8 (d,  $J_{\text{CF}} = 24.8$  Hz), 99.2 (d,  $J_{\text{CF}} = 25.7$  Hz), 89.6.

**(E)-6-Fluoro-3-[2-(1H-tetrazol-5-yl)vinyl]-1H-indole (58).** 58 was synthesized from nitrile **56-trans** (358 mg, 1.92 mmol) following the general synthetic method C with a reaction time of 18 h. Yellowish powder, yield 282 mg (64%). Mp 228–230 °C. LC/MS  $t_R$  = 5.1 min,  $m/z$  [MH<sup>+</sup>] 230. <sup>1</sup>H NMR  $\delta$  11.69 (1H, bs, indole-H1), 7.87–7.89 (2H, m, 2 ArH), 7.78 (1H, d,  $J$  = 16.7 Hz, HC=CH), 7.22 (1H, dd,  $J$  = 9.8, 2.3 Hz, ArH), 7.02 (1H, overlapped d, HC=CH), 7.01 (1H, overlapped, ArH). <sup>13</sup>C NMR  $\delta$  159.7 (d,  $J_{CF}$  = 235.5 Hz), 155.2 (tetrazole-CS), 137.7 (d,  $J_{CF}$  = 12.39 Hz), 132.2, 130.5, 122.2, 121.1 (d,  $J_{CF}$  = 9.53 Hz), 112.7, 109.4 (d,  $J_{CF}$  = 23.8 Hz), 104.9, 99.0 (d,  $J_{CF}$  = 25.8 Hz).

**(E)-3-(6-Fluoro-1H-indol-3-yl)acrylic Acid (61).** A solution of potassium hydroxide (66 mg, 1.18 mmol) in H<sub>2</sub>O (1.5 mL) was added to a solution of ester **50** in ethanol (3 mL), and the cloudy mixture was heated at reflux temperature for 1 h. The clear solution obtained was cooled to room temperature and then partitioned between ethyl acetate and 1 M aqueous citric acid. The aqueous layer was extracted twice with ethyl acetate, and the combined organic layers were dried over MgSO<sub>4</sub>. Purification by flash chromatography followed by precipitation as described above yielded the title compound as a yellowish solid, 75 mg (82%). Mp 201–203 °C. LC/MS  $t_R$  = 5.1 min,  $m/z$  [MH<sup>+</sup>] 206, 188. <sup>1</sup>H NMR  $\delta$  12.23 (1H, bs), 11.73 (1H, bs), 7.88 (1H, d,  $J$  = 2.7 Hz, ArH), 7.82 (1H, dd,  $J$  = 8.8, 5.4 Hz, ArH), 7.74 (1H, d,  $J$  = 16.0 Hz, HC=CH), 7.21 (1H, dd,  $J$  = 9.7, 2.4 Hz, ArH), 6.98 (1H, dt,  $^3J$  = 9.2 Hz,  $^4J$  = 2.4 Hz, ArH), 6.27 (1H, d,  $J$  = 16.0 Hz, HC=CH). <sup>13</sup>C NMR  $\delta$  169.0 (C=O), 159.7 (d,  $J_{CF}$  = 235.5 Hz), 138.6, 137.9 (d,  $J_{CF}$  = 12.4 Hz), 132.4, 122.3, 121.5 (d,  $J_{CF}$  = 10.5 Hz), 113.2, 112.3, 109.6 (d,  $J_{CF}$  = 23.8 Hz), 99.0 (d,  $J_{CF}$  = 24.8 Hz).

**Cellular Assay.** *Cell Line.* P815B cells were transfected with a plasmid construct encoding mouse TDO2. Clone P185B-mTDO clone 12 which overexpresses TDO was selected and used for the cellular assay.

*Assay.* The assay was performed in 96-well flat bottom plates seeded with  $2 \times 10^5$  cells in a final volume of 200  $\mu$ L. To determine the TDO inhibitory potency of the synthesized molecules, the cells were incubated for 8 h at 37 °C in HBSS (Hanks' balanced salt solution, Invitrogen) supplemented with 80  $\mu$ M L-tryptophan and 2, 20, or 200  $\mu$ M of the studied compound. To determine the IC<sub>50</sub>, the cells were incubated for 8 h at 37 °C in HBSS supplemented with 80  $\mu$ M L-tryptophan and a titration of the compound ranging from 0.3 to 80  $\mu$ M or from 1.5 to 400  $\mu$ M. The plates were then centrifuged for 10 min at 300g, and 150  $\mu$ L of the supernatant was collected. The wells were preserved for cell viability evaluation. The supernatant was analyzed by HPLC to measure the concentration of residual tryptophan and produced kynurenine, based on the retention time and the UV absorption (280 nm for tryptophan, 360 nm for kynurenine). For the HPLC analysis, an amount of 50  $\mu$ L of supernatant was mixed with 500  $\mu$ L of acetonitrile to precipitate the proteins. After centrifugation, the supernatant was collected, concentrated on a centrifugal vacuum concentrator, and resuspended in a final volume of 100  $\mu$ L of water, and an amount of 90  $\mu$ L was injected onto an Onyx Monolithic C18 column (Phenomenex). For each compound, the percentages of inhibition of tryptophan catabolism and kynurenine production by the compounds were calculated in reference to the maximal activity in the absence of potential inhibitor. The cell viability was estimated by a MTT assay. To that end, an amount of 50  $\mu$ L of culture medium (Iscove medium with 10% FCS and amino acids) was added to the wells together with 50  $\mu$ L of MTT. After 3–4 h of incubation at 37 °C, an amount of 100  $\mu$ L of SDS/DMF was added to dissolve the crystals of formazan blue and the absorbance was measured at 570 nm/650 nm after overnight incubation at 37 °C.

**Kinetic Analysis.** The coding region (Met<sub>1</sub>-Asp<sub>406</sub>) of human TDO (hTDO) gene was cloned into a derivative of plasmid pET9 (Novagen). The recombinant plasmid, pET<sub>hTDO</sub>, was transformed into the bacterial strain BL21 AI (Invitrogen). The transformed cells were grown to an optical density of 1 at 600 nm, on a rotary shaker (37 °C and 220 rpm), in LB medium supplemented with kanamycin

sulfate (25  $\mu$ g·mL<sup>-1</sup>), L-tryptophan (50  $\mu$ g·mL<sup>-1</sup>), and bovine hemin (40  $\mu$ M, Sigma). The culture was cooled in a water/ice bath and supplemented again with kanamycin sulfate (25  $\mu$ g·mL<sup>-1</sup>), L-tryptophan (50  $\mu$ g·mL<sup>-1</sup>), and bovine hemin (40  $\mu$ M). The expression of hTDO was induced by the addition of arabinose (0.2% w/v). Induced cells were grown for 20 h (20 °C and 60 rpm). Cell suspension (50 mL) were centrifuged (6000g), and the pellet was resuspended in 10 mL of 50 mM potassium phosphate buffer, pH 7.5, containing KCl (150 mM), L-tryptophan (1 mM), bovine hemin (10  $\mu$ M), and a cocktail of protease inhibitors (complete EDTA free, Roche Applied Science) and disrupted with a French press. The extract was clarified by centrifugation (20000g) and filtration on a 0.22  $\mu$ m filter. The buffer of the extract was then exchanged to 50 mM potassium phosphate buffer, pH 7.5, using a HiPrep 26/10 desalting column (GE Healthcare). Aliquots were frozen in liquid nitrogen and kept at –80 °C until use.

To measure the TDO activity, the reaction mixture contained potassium phosphate buffer (50 mM, pH 7.5), ascorbic acid (20 mM), methylene blue (10  $\mu$ M), catalase (500 units·mL<sup>-1</sup>, from bovine liver, Sigma), and L-Trp without or with hTDO inhibitor at the indicated concentrations. The reaction was initiated by the addition of 10  $\mu$ L of recombinant hTDO extract (~3  $\mu$ g of total proteins) to 190  $\mu$ L of prewarmed (37 °C) reaction mixture. The reaction was conducted at 37 °C for 2 and 4 min and stopped by the addition of 40  $\mu$ L of 30% (w/v) trichloroacetic acid. To convert N-formylkynurenine into kynurenine, the reaction mixture was incubated at 65 °C for 30 min. Then 125  $\mu$ L of the reaction mixture was mixed with 125  $\mu$ L of 2% (w/v) 4-(dimethylamino)-benzaldehyde in acetic acid and incubated for 10 min at room temperature. Kynurenine concentrations were determined by measuring the absorbance at 480 nm. A standard curve was made with pure kynurenine. The rate of catalysis was calculated from the increase of kynurenine concentration between 2 and 4 min. The TDO activity was measured as described above at L-Trp concentrations of 50, 100, 200, 400, and 800  $\mu$ M using three different inhibitor concentrations. Data were fitted using the Prism software (GraphPad Software, Inc.).

**Solubility Evaluation.** The solubility was evaluated using Multi-screen HTS-PCF filter plates from Millipore following a protocol adapted from the Millipore application note ("Quantitative Method to Determine Drug Aqueous Solubility: Optimization and Correlation to Standard Methods" Thomas Onofrey and Greg Kazan, <http://www.millipore.com/techpublications/tech1/an1730en00>) at pH 1.0 (HCl 0.1 M, NaCl 20 mM), 7.4 (phosphate buffer 50 mM, NaCl 30 mM), and 9.0 (boric acid 0.1 M, NaCl 20 mM) and with a final DMSO concentration of 2.5%. The filtrate was analyzed using an Agilent 1100 series LC/MSD trap system with UV detection at 254 nm equipped with a C<sub>18</sub> Zorbax SB column (100 mm  $\times$  3 mm, 3.5  $\mu$ m) and following a gradient (flow rate of 0.5 mL·min<sup>-1</sup>) of acetonitrile in aqueous acetic acid 0.1% (v/v): from 5% to 95% of acetonitrile in 5 min, holding for 3 min, then reversing to 5% of acetonitrile in 0.1 min and holding for an additional 5.4 min.

**Bioavailability.** DBA/2 mice were given **22** (pH 2.5), **51** (pH 9), or **49** (pH 9) solubilized in the drinking water (1 mg·mL<sup>-1</sup>). The average water consumption was 4.0 mL·day<sup>-1</sup> by animal. At days 0, 1, 2 and 7, blood of three mice was collected from the orbital sinus. After incubation overnight at 4 °C and centrifugation at 11000g during 10 min, the serum was collected. The concentrations of the studied molecule, tryptophan, and kynurenine were measured by HPLC.

**Molecular Modeling.** Molecular modeling studies were carried out on a Linux workstation. The compounds were built using the SKETCH module implemented in SYBYL (version 8.0).<sup>53</sup> Docking was performed using the 3D coordinates of TDO (PDB code 2NW9) with the help of the automated GOLD program<sup>36</sup> (active site definition: residues within 7 Å around 6-fluorotryptophan). In order to take protein flexibility into account, the enzyme–inhibitor complexes were optimized using the MINIMIZE module. The minimization process uses the

Powell method with the Tripos force field (dielectric constant 1r) to reach a final convergence of  $0.01 \text{ kcal} \cdot \text{mol}^{-1}$ .

**Selectivity Assays.** *Enzymes.* The inhibitory potencies of **58** on IDO and MAO-A and -B were assessed as described previously by Dolusić et al.<sup>25,26</sup> and Reniers et al.<sup>54,55</sup> for IDO and for MAO-A and -B, respectively.

*Receptors and Transporters.* Receptor binding assays were performed at CEREP (France). Briefly, the specific ligand binding to the receptors was defined as the difference between the total binding and the nonspecific binding determined in the presence of an excess of unlabeled ligand. The results are expressed as a percent inhibition of control specific binding ( $100 - (\text{measured specific binding}/\text{control specific binding}) \times 100$ ) obtained in the presence of **58**.

## ■ ASSOCIATED CONTENT

**S** **Supporting Information.** Detailed synthesis and characterization of all reported derivatives. This material is available free of charge via the Internet at <http://pubs.acs.org>.

## ■ AUTHOR INFORMATION

### Corresponding Author

\*Phone: +32 81 72 42 90. Fax: +32 81 72 42 38. E-mail: [raphael.frederick@fundp.ac.be](mailto:raphael.frederick@fundp.ac.be).

## ■ ACKNOWLEDGMENT

The authors thank Sara Modaffari, Christelle Vancaeynest, and Debora Piccolo, Jérémy Maury, and Jérémy Reniers for their assistance. R.F. is greatly indebted to the Fonds de la Recherche Scientifique—FNRS for the award of a postdoctoral grant. This project was funded in part by Télévie (FNRS Grant 7.4.543.07).

## ■ ABBREVIATIONS USED

TDO, tryptophan 2,3-dioxygenase; IDO, indoleamine 2,3-dioxygenase; NAD, nicotinamide dinucleotide; L-Trp, L-tryptophan; 5-HT, serotonin; TMSCHN<sub>2</sub>, trimethylsilyldiazomethane; NMP, N-methyl-2-pyrrolidone; DIBAL, diisobutylaluminum hydride

## ■ REFERENCES

- (1) Rafice, S. A.; Chauhan, N.; Efimov, I.; Basran, J.; Raven, E. L. Oxidation of L-tryptophan in biology: a comparison between tryptophan 2,3-dioxygenase and indoleamine 2,3-dioxygenase. *Biochem. Soc. Trans.* **2009**, *37*, 408–412.
- (2) Sono, M.; Roach, M. P.; Coulter, E. D.; Dawson, J. H. Heme-containing oxygenases. *Chem. Rev.* **1996**, *96*, 2841–2888.
- (3) Stone, T. W.; Darlington, L. G. Endogenous kynurenes as targets for drug discovery and development. *Nat. Rev. Drug Discovery* **2002**, *1*, 609–620.
- (4) Forouhar, F.; Anderson, J. L.; Mowat, C. G.; Vorobiev, S. M.; Hussain, A.; Abashidze, M.; Bruckmann, C.; Thackray, S. J.; Seetharaman, J.; Tucker, T.; Xiao, R.; Ma, L. C.; Zhao, L.; Acton, T. B.; Montelione, G. T.; Chapman, S. K.; Tong, L. Molecular insights into substrate recognition and catalysis by tryptophan 2,3-dioxygenase. *Proc. Natl. Acad. Sci. U.S.A.* **2007**, *104*, 473–478.
- (5) Kotake, Y.; Masayama, I. The intermediary metabolism of tryptophan. XVIII. The mechanism of formation of kynurenine from tryptophan. *Z. Physiol. Chem.* **1936**, *243*, 237–244.
- (6) Knox, W. E.; Mehler, A. H. The conversion of tryptophan to kynurenine in liver. I. The coupled tryptophan peroxidase–oxidase system forming formylkynurenine. *J. Biol. Chem.* **1950**, *187*, 419–430.

- (7) Leeds, J. M.; Brown, P. J.; McGeehan, G. M.; Brown, F. K.; Wiseman, J. S. Isotope effects and alternative substrate reactivities for tryptophan 2,3-dioxygenase. *J. Biol. Chem.* **1993**, *268*, 17781–17786.

- (8) Katz, J. B.; Muller, A. J.; Prendergast, G. C. Indoleamine 2,3-dioxygenase in T-cell tolerance and tumoral immune escape. *Immunol. Rev.* **2008**, *222*, 206–221.

- (9) Hwu, P.; Du, M. X.; Lapointe, R.; Do, M.; Taylor, M. W.; Young, H. A. Indoleamine 2,3-dioxygenase production by human dendritic cells results in the inhibition of T cell proliferation. *J. Immunol.* **2000**, *164*, 3596–3599.

- (10) Mellor, A. Indoleamine 2,3 dioxygenase and regulation of T cell immunity. *Biochem. Biophys. Res. Commun.* **2005**, *338*, 20–24.

- (11) Munn, D. H.; Shafizadeh, E.; Attwood, J. T.; Bondarev, I.; Pashine, A.; Mellor, A. L. Inhibition of T cell proliferation by macrophage tryptophan catabolism. *J. Exp. Med.* **1999**, *189*, 1363–1372.

- (12) Munn, D. H.; Zhou, M.; Attwood, J. T.; Bondarev, I.; Conway, S. J.; Marshall, B.; Brown, C.; Mellor, A. L. Prevention of allogeneic fetal rejection by tryptophan catabolism. *Science* **1998**, *281*, 1191–1193.

- (13) Terness, P.; Bauer, T. M.; Rose, L.; Dufter, C.; Watzlik, A.; Simon, H.; Opelz, G. Inhibition of allogeneic T cell proliferation by indoleamine 2,3-dioxygenase-expressing dendritic cells: mediation of suppression by tryptophan metabolites. *J. Exp. Med.* **2002**, *196*, 447–457.

- (14) Uyttenhove, C.; Pilotte, L.; Theate, I.; Stroobant, V.; Colau, D.; Parmentier, N.; Boon, T.; Van den Eynde, B. J. Evidence for a tumoral immune resistance mechanism based on tryptophan degradation by indoleamine 2,3-dioxygenase. *Nat. Med.* **2003**, *9*, 1269–1274.

- (15) Brandacher, G.; Perathoner, A.; Ladurner, R.; Schneeberger, S.; Obrist, P.; Winkler, C.; Werner, E. R.; Werner-Felmayer, G.; Weiss, H. G.; Gobel, G.; Margreiter, R.; Konigsrainer, A.; Fuchs, D.; Amberger, A. Prognostic value of indoleamine 2,3-dioxygenase expression in colorectal cancer: effect on tumor-infiltrating T cells. *Clin. Cancer Res.* **2006**, *12*, 1144–1151.

- (16) Munn, D. H.; Mellor, A. L. Indoleamine 2,3-dioxygenase and tumor-induced tolerance. *J. Clin. Invest.* **2007**, *117*, 1147–1154.

- (17) Okamoto, A.; Nikaido, T.; Ochiai, K.; Takakura, S.; Saito, M.; Aoki, Y.; Ishii, N.; Yanaiharu, N.; Yamada, K.; Takikawa, O.; Kawaguchi, R.; Isonishi, S.; Tanaka, T.; Urashima, M. Indoleamine 2,3-dioxygenase serves as a marker of poor prognosis in gene expression profiles of serous ovarian cancer cells. *Clin. Cancer Res.* **2005**, *11*, 6030–6039.

- (18) Prendergast, G. C. Immune escape as a fundamental trait of cancer: focus on IDO. *Oncogene* **2008**, *27*, 3889–3900.

- (19) Muller, A. J.; DuHadaway, J. B.; Donover, P. S.; Sutanto-Ward, E.; Prendergast, G. C. Inhibition of indoleamine 2,3-dioxygenase, an immunoregulatory target of the cancer suppression gene Bin1, potentiates cancer chemotherapy. *Nat. Med.* **2005**, *11*, 312–319.

- (20) Muller, A. J.; Malachowski, W. P.; Prendergast, G. C. Indoleamine 2,3-dioxygenase in cancer: targeting pathological immune tolerance with small-molecule inhibitors. *Expert Opin. Ther. Targets* **2005**, *9*, 831–849.

- (21) Muller, A. J.; Prendergast, G. C. Indoleamine 2,3-dioxygenase in immune suppression and cancer. *Curr. Cancer Drug Targets* **2007**, *7*, 31–40.

- (22) Lob, S.; Konigsrainer, A.; Zieker, D.; Brucher, B. L.; Rammensee, H. G.; Opelz, G.; Terness, P. IDO1 and IDO2 are expressed in human tumors: levo- but not dextro-1-methyl tryptophan inhibits tryptophan catabolism. *Cancer Immunol. Immunother.* **2009**, *58*, 153–157.

- (23) Macchiarulo, A.; Camaioni, E.; Nuti, R.; Pellicciari, R. High-lights at the gate of tryptophan catabolism: a review on the mechanisms of activation and regulation of indoleamine 2,3-dioxygenase (IDO), a novel target in cancer disease. *Amino Acids* **2009**, *37*, 219–229.

- (24) Rohrig, U. F.; Awad, L.; Grosdidier, A.; Larriue, P.; Stroobant, V.; Colau, D.; Cerundolo, V.; Simpson, A. J.; Vogel, P.; Van den Eynde, B. J.; Zoete, V.; Michielin, O. Rational design of indoleamine 2,3-dioxygenase inhibitors. *J. Med. Chem.* **2010**, *53*, 1172–1189.

- (25) Dolusić, E.; Larriue, P.; Blanc, S.; Sapunarić, F.; Norberg, B.; Moineaux, L.; Colette, D.; Stroobant, V.; Pilotte, L.; Colau, D.; Ferain, T.; Fraser, G.; Galeni, M.; Frere, J. M.; Masereel, B.; Van den Eynde, B.

Wouters, J.; Frederick, R. Indol-2-yl ethanones as novel indoleamine 2,3-dioxygenase (IDO) inhibitors. *Bioorg. Med. Chem.* **2011**, *19*, 1550–1561.

(26) Dolušić, E.; Larrieu, P.; Blanc, S.; Sapunarić, F.; Pouyez, J.; Moineaux, L.; Colette, D.; Stroobant, V.; Pilotte, L.; Colau, D.; Ferain, T.; Fraser, G.; Galleni, M.; Frère, J.-M.; Masereel, B.; Van den Eynde, B.; Wouters, J.; Frédérick, R. Discovery and preliminary SARs of keto-indoles as novel indoleamine 2,3-dioxygenase (IDO) inhibitors. *Eur. J. Med. Chem.* **2011**, *46*, 3058–3065.

(27) Van den Eynde, B.; Pilotte, L.; De Plaen, E. Tryptophan Catabolism in Cancer Treatment and Diagnosis. WO2010008427, 2010.

(28) Civen, M.; Knox, W. E. The specificity of tryptophan analogues as inducers, substrates, inhibitors, and stabilizers of liver tryptophan pyrrolase. *J. Biol. Chem.* **1960**, *235*, 1716–1718.

(29) Eguchi, N.; Watanabe, Y.; Kawanishi, K.; Hashimoto, Y.; Hayaishi, O. Inhibition of indoleamine 2,3-dioxygenase and tryptophan 2,3-dioxygenase by beta-carboline and indole derivatives. *Arch. Biochem. Biophys.* **1984**, *232*, 602–609.

(30) Frieden, E.; Westmark, G. W.; Schor, J. M. Inhibition of tryptophan pyrrolase by serotonin, epinephrine and tryptophan analogs. *Arch. Biochem. Biophys.* **1961**, *92*, 176–182.

(31) Madge, D. G.; Hazelwood, R. I.; Jones, H. T.; Salter, M. Novel tryptophan dioxygenase inhibitors and combined tryptophan dioxygenase/5-HT reuptake inhibitors. *Bioorg. Med. Chem. Lett.* **1996**, *6*, 857–860.

(32) Reinhard, J. F., Jr.; Flanagan, E. M.; Madge, D. J.; Iyer, R.; Salter, M. Effects of 540C91 [(E)-3-[2-(4'-pyridyl)-vinyl]-1H-indole], an inhibitor of hepatic tryptophan dioxygenase, on brain quinolinic acid in mice. *Biochem. Pharmacol.* **1996**, *51*, 159–163.

(33) Salter, M.; Hazelwood, R.; Pogson, C. I.; Iyer, R.; Madge, D. J. The effects of a novel and selective inhibitor of tryptophan 2,3-dioxygenase on tryptophan and serotonin metabolism in the rat. *Biochem. Pharmacol.* **1995**, *49*, 1435–1442.

(34) Salter, M.; Hazelwood, R.; Pogson, C. I.; Iyer, R.; Madge, D. J.; Jones, H. T.; Cooper, B. R.; Cox, R. F.; Wang, C. M.; Wiard, R. P. The effects of an inhibitor of tryptophan 2,3-dioxygenase and a combined inhibitor of tryptophan 2,3-dioxygenase and 5-HT reuptake in the rat. *Neuropharmacology* **1995**, *34*, 217–227.

(35) Zhang, Y.; Kang, S. A.; Mukherjee, T.; Bale, S.; Crane, B. R.; Begley, T. P.; Ealick, S. E. Crystal structure and mechanism of tryptophan 2,3-dioxygenase, a heme enzyme involved in tryptophan catabolism and in quinolinate biosynthesis. *Biochemistry* **2007**, *46*, 145–155.

(36) Jones, G.; Willett, P.; Glen, R. C.; Leach, A. R.; Taylor, R. Development and validation of a genetic algorithm for flexible docking. *J. Mol. Biol.* **1997**, *267*, 727–748.

(37) Delano, W. L. The PyMOL Molecular Graphics System on World Wide Web. <http://www.pymol.org/> (accessed June 29, 2011).

(38) Lefoix, M.; Daillant, J.-P.; Routier, S.; Mérour, J.-Y.; Gillaizeau, I.; Coudert, G. Versatile and convenient methods for the synthesis of C-2 and C-3 functionalised 5-aza-indoles. *Synthesis* **2005**, *20*, 3581–3588.

(39) Lebel, H.; Davi, M.; Díez-González, S.; Nolan, S. P. Copper–carbene complexes as catalysts in the synthesis of functionalized styrenes and aliphatic alkenes. *J. Org. Chem.* **2007**, *72*, 144–149.

(40) Gromov, S. P.; Vedernikov, A. I.; Ushakov, E. N.; Lobova, N. A.; Botsmanova, A. A.; Kuz'mina, L. G.; Churakov, A. V.; Strelenko, Y. A.; Alfimov, M. V.; Howard, J. A. K.; Johnels, D.; Edlund, U. G. Novel supramolecular charge-transfer systems based on bis(18-crown-6)stilbene and viologen analogues bearing two ammonioalkyl groups. *New J. Chem.* **2005**, *29*, 881–894.

(41) Juby, P. F.; Hudyma, T. W. Preparation and antiinflammatory properties of some 1-substituted 3-(5-tetrazolylmethyl)indoles and homologs. *J. Med. Chem.* **1969**, *12*, 396–401.

(42) Vereshchagin, L. I.; Petrov, A. V.; Kizhnyaev, V. N.; Pokatilov, F. A.; Smirnov, A. I. Polynuclear nonfused bis(1,3,4-oxadiazole)-containing systems. *Russ. J. Org. Chem.* **2006**, *42*, 1049–1055.

(43) Grimster, N. P.; Gauntlett, C.; Godfrey, C. R. A.; Gaunt, M. J. Palladium-catalyzed intermolecular alkenylation of indoles by solvent-controlled regioselective C–H functionalization. *Angew. Chem., Int. Ed.* **2005**, *44*, 3125–3129.

(44) Moriya, T.; Hagio, K.; Yoneda, N. Preparation and reactions of 3-(aminomethylene)-3H-indoles. *Chem. Pharm. Bull.* **1980**, *28*, 1711–1721.

(45) Sørensen, U. S.; Pombo-Villar, E. Copper-free palladium-catalyzed Sonogashira-type coupling of aryl halides and 1-aryl-2-(trimethylsilyl)acetylenes. *Tetrahedron* **2005**, *61*, 2697–2703.

(46) Sundberg, R. G.; Luis, J. G.; Parton, R. L.; Schreiber, S.; Srinivasan, P. C.; Lamb, P.; Forcier, P.; Bryan, R. B. Chloroacetamide photocyclization of indole derivatives. Synthesis, stereochemistry, and crystal structure of 3,7-methano-3-azacycloundecino[5,4-b]indole (deethylquebrachamine) derivatives. *J. Org. Chem.* **1978**, *23*, 4859–4865.

(47) Sureshbabu, V. V.; Vasantha, B.; Hemantha, H. P. Synthesis of N-Fmoc-protected amino alkyl thiocyanates/selenocyanates and their application in the preparation of 5-substituted S/Se-linked tetrazoles. *Synthesis* **2011**, *9*, 1447–1455.

(48) ACD/Structure Designer, version 12.0; Advanced Chemistry Development: Toronto, Ontario, Canada, 2010; [www.acdlabs.com](http://www.acdlabs.com).

(49) Herr, R. J. 5-Substituted-1H-tetrazoles as carboxylic acid isosteres: medicinal chemistry and synthetic methods. *Bioorg. Med. Chem.* **2002**, *10*, 3379–3393.

(50) Gaspari, P.; Banerjee, T.; Malachowski, W. P.; Muller, A. J.; Prendergast, G. C.; DuHadaway, J.; Bennett, S.; Donovan, A. M. Structure–activity study of brassinin derivatives as indoleamine 2,3-dioxygenase inhibitors. *J. Med. Chem.* **2006**, *49*, 684–692.

(51) Yue, E. W.; Douty, B.; Wayland, B.; Bower, M.; Liu, X.; Leffert, L.; Wang, Q.; Bowman, K. J.; Hansbury, M. J.; Liu, C.; Wei, M.; Li, Y.; Wynn, R.; Burn, T. C.; Koblisch, H. K.; Fridman, J. S.; Metcalf, B.; Scherle, P. A.; Combs, A. P. Discovery of potent competitive inhibitors of indoleamine 2,3-dioxygenase with in vivo pharmacodynamic activity and efficacy in a mouse melanoma model. *J. Med. Chem.* **2009**, *52*, 7364–7367.

(52) Boularot, A.; Giglione, C.; Petit, S.; Duroc, Y.; Alves de Sousa, R.; Larue, V.; Cresteil, T.; Dardel, F.; Artaud, I.; Meinel, T. Discovery and refinement of a new structural class of potent peptide deformylase inhibitors. *J. Med. Chem.* **2007**, *50*, 10–20.

(53) SYBYL, version 8.0; Tripos Inc. (South Hanley Rd, St. Louis, MO, 63144, U.S.).

(54) Frederick, R.; Dumont, W.; Ooms, F.; Aschenbach, L.; Van der Schyf, C. J.; Castagnoli, N.; Wouters, J.; Krief, A. Synthesis, structural reassignment, and biological activity of type B MAO inhibitors based on the 5H-indeno[1,2-c]pyridazin-5-one core. *J. Med. Chem.* **2006**, *49*, 3743–3747.

(55) Reniers, J.; Robert, S.; Frederick, R.; Masereel, B.; Vincent, S.; Wouters, J. Synthesis and evaluation of beta-carboline derivatives as potential monoamine oxidase inhibitors. *Bioorg. Med. Chem.* **2011**, *19*, 134–144.